2014

Fatigue Based Structural Design Exploration via Engineering Data Analytics

Hao Li
Wright State University

Fatigue Based Structural Design Exploration via Engineering Data Analytics

A thesis submitted in partial fulfillment
of the requirement for the degree of
Master of Science in Engineering

By

Hao Li

B.S., Taiyuan University of Technology, China, 2012

2014
Wright State University

WRIGHT STATE UNIVERSITY
GRADUATE SCHOOL

July 18, 2014

I HEREBY RECOMMEND THAT THE THESIS PREPARED UNDER MY SUPERVISION BY **Hao Li** ENTITLED **Fatigue Based Structural Design Exploration via Engineering Data Analytics** BE ACCEPTED IN PARTIAL FULFILLMENT OF THE REQUIREMENTS FOR THE DEGREE OF **Master of Science in Engineering**.

_____

Ha-Rok Bae, Ph.D.
Thesis Director

_____

George P. G. Huang, Ph.D., P.E.
Chair, Department of Mechanical and
Materials Engineering

Committee on Final Examination:

_____

Ha-Rok Bae, Ph.D.

_____

Zifeng Yang, Ph.D.

_____

Sanjiv Kumar Sinha, Ph.D.

_____

Robert E. W. Fyffe, Ph.D.
Vice President for Research and
Dean of the Graduate School

ABSTRACT

Li, Hao. M.S.Egr., Department of Mechanical and Materials Engineering, Wright State University, 2014. *Fatigue Based Structural Design Exploration via Engineering Data Analytics.*

In manufacturing industry, a successful machine development requires the durability of structure components to meet fatigue life targets. The typical way to obtain fatigue design loads for conceptual design exploration is based on hand calculations or historical data to capture envelopes of expected system responses, which may not guarantee to capture actual damaging loads. In this study, a new approach is developed to extract a fatigue design load set directly from measured load data for a conceptual design exploration. The proposed framework integrates the techniques from data analytics and physics based engineering mechanics to amplify and detect fundamental damaging load patterns. Also, a practical Taguchi optimization method is proposed by using a moving window strategy to minimize the computational cost of design exploration. An industrial scale structural problem, a front linkage structure of a hydraulic excavator, is presented to demonstrate the effectiveness of the proposed methodologies.

Table of Contents

List of Figures

List of Tables

Acknowledgment

First of all, I would like to express my gratitude to my advisor Dr. Ha-Rok Bae, for his patience and guidance on my research work in graduate school. I learned a lot from him not only academically but also spiritually. I would also like to thank my committee members, Dr. Zifeng Yang and Dr. Sanjiv Kumar Sinha, for sparing their precious time to serve on my committee and providing me valuable feedback.

Additionally, I would like to thank CEPRO members, Josh, Anoop, Corey, Koorosh and James, for their kind help, valuable advice and helpful feedback. I enjoy the time working with them. I would also like to extend my special thanks to my parents, Mr. Zhijiang Li and Mrs. Lan Qu, for their endless love and encouragement. Without their support, I cannot imagine I can get to this point.

1. Introduction

1.1 Background and motivation

Before developing a new machine in the heavy earth moving industries, the full spectrum of product applications and critical needs are surveyed by a wide range of customers. After the survey, design targets are analyzed and cascaded through all subsystems of the new machine to be built. Among all the design targets, engineers should be confident about the structural durability assessment, which makes structural fatigue life target one of the most significant design objectives for a structural system. Traditionally, the common way to assess structural durability is by performing physical dynamic tests with a full scale prototype machine at a test ground at every stage of design development. However, it is time consuming and expensive. Therefore, using powerful advanced simulations, a virtual design exploration process [1, 2] is employed to reduce dependency on physical tests. The amount of measured data is often immense because a typical sampling rate of a test measurement is around several hundred hertz, which makes it difficult to be used for an iterative simulation based concept design exploration in the virtual design exploration. Instead of using measured load data directly, static design loads extracted from worst cases of machine operations are often used for the sake of structural durability assessments, especially for a concept design evaluation. Achieving successful machine development depends on a good concept design, since it can reduce any budgetary or project schedule risk arising from unnecessary physical tests and design alterations. It is obvious that how well the fatigue design loads represent the measured load data leads to how accurate the durability evaluation in concept design exploration.

Based on potential extreme cases of machine operations, the typical way to get the fatigue design loads is mainly based on experience and simple hand calculations. However, these design loads may not be appropriate to account for all critical fatigue load contents during actual operations. Thus, an alternative way to extract representative fatigue design loads directly from measured loads is desirable.

Several load extraction methods have been proposed by researchers [3-5] that can generate static design loads from measured loads for fast design iterations. Kang et al. [3] developed an analytical method to transform dynamic loads into equivalent static loads based on modal analysis. However, the static loads are aimed at reproducing equivalent displacement fields, not fatigue damage. Based on the fatigue history wavelet transform [6], Adbullah et al. [7] developed the Wavelet Bump Extraction (WBE) algorithm to find fatigue design loads. In this method, the signal is converted from the time domain to the frequency domain using the Fast Fourier Transform method. The frequency domain signal is decomposed into multiple wavelets in which each wavelet covers frequency regions of specific failure locations. Then, the fatigue damage events or bumps are identified such that they produce equivalent signal statistics and fatigue damage to the original signal. In practical cases, however, WBE is ineffective to interpret the critical features of the fatigue loads method when it deals with many damage locations related with different frequency ranges.

Thus, there are mainly two concerns in the process of load extraction. One of them is how to capture the completeness and uniqueness of fundamental fatigue load patterns directly from the complex and large amount of test data. Once the fundamental fatigue load patterns are obtained, how to convert the fundamental load information into

practical static fatigue design loads and how to make them applicable is another challenge. It is desirable to have a new approach to deal with these challenges to get the fatigue design loads.

Taguchi design was widely used in the manufacturing industry as a quality control and design tool in many US and European industries since the 1980s. According to Taguchi, quality loss is defined as the total loss imparted to the society from the time a product is shipped to the customer. In order to minimize loss, products should be designed to achieve optimal performance with minimal variation in this performance. Taguchi's fundamental concept rests on the importance of economically achieving high quality, low variability and consistency of functional performance [8, 9]. However, the typical way for Taguchi design needs a lot of professional judgments and individual experience. This manual process will greatly affect the effectiveness for product development. Thus, a programming package is needed to transfer this manual process into an automatic one. How to achieve the professional judgments and individual experience by computational power is the challenge for this process.

1.2 Thesis organization

In this study, there are basically two main approaches proposed. One is the new fatigue design load development method via Engineering Data Analytics (EDA) and optimization techniques. The other one is the Taguchi design toolkit using moving window strategies.

The fatigue design load development method is proposed based on data analytics process and optimization techniques, coupled with fatigue mechanics to amplify and

capture fundamental damaging load patterns. First, based on the engineering data analytics proposed by Bae at al. [10], fundamental fatigue load patterns are identified from large amounts of measured load data. Hidden patterns of the fundamental fatigue loads are amplified by damage-based sensitivity. Then, in order to get applicable static fatigue design loads with the identified fundamental fatigue load patterns, inverse optimization formulations are set up in a two-stage process to determine the optimum scales and frequencies. In order to obtain physically-valid initial guesses of the inverse problems, data analytics and pre-optimization studies are performed.

The paper is organized in the following manner: Chapter 2 is the literature review about the typical approach used for inverse analysis, durability evaluation of concept designs and Taguchi design process. Chapter 3 introduces the proposed Engineering Data Analytics (EDA) methods for fatigue design load development along with the automatic Taguchi design framework. This is followed by numerical demonstrations and case studies with a common structural component, an I-section cantilever beam, and an industrial large-scale structure, the front linkage of a hydraulic excavator in Chapter 4. Chapter 5 will conclude with a summary of the research findings and potential next topics.

2. Literature review

2.1 Inverse analysis

In forward problems, or direct problems, analytical or numerical responses for given system are determined with known initial and boundary conditions. The key point here is that the responses of interests are computed directly as functions of input and there is no need for the measurements or targets. Mathematically, forward problems are well-posed problems. Unique and stable solution exists and the globally defined solution exists.

For inverse problems, basic requirements for solution of these problems are appropriate targets and a mathematical model. Based on the type of targets, inverse problem can be classified as these two types [11]:

- Inverse measurement problems
- Inverse design problems

In inverse measurement problems, the dependent variable might be measured at many discrete times at one or more positions, which leads to the error of measurements. While for the inverse design problems, the targets are known exactly or obtained by numerical method, such as finite element or finite differences, and do not rely on empirically gathered data. Inverse problems are ill-posed, solution is not unique and stable. Also, there are infinite approximate solutions around an optimum. Thus, if they are solved in the straightforward manner, it happens a lot for the solution to be large oscillations or meaningless. Based on the type of information that is being sought in the

solution procedure, there are basically three different types of inverse problems [12], which are shown schematically in Figure 2.1:

- Parameter inverse problem, when parameters in model is to be found;
- Backward or retrospective problem, when initial conditions are to be found;
- Boundary inverse problem, when some missing information at the boundary of a domain is to be found.

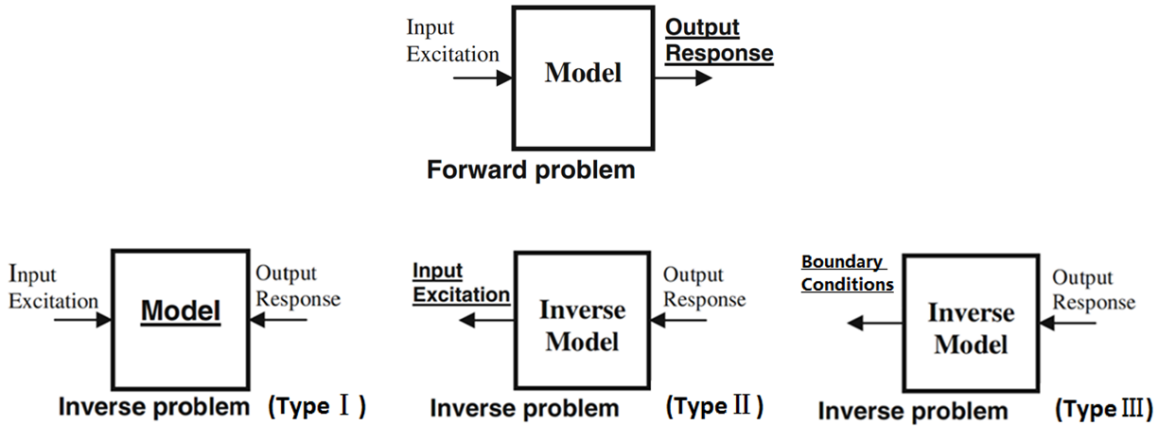

Figure 2.1: Forward and inverse problem

In the paper by Beck et al. [11], existed general methodologies for inverse measurement problems of parameter estimation are reviewed. Different objective functions are selected based on different types of measurement errors. For uncorrelated errors that are additive, zero mean and constant variance with a Gaussian distribution, an ordinary least squares objective function with weighting function is often applied shown in the following equation:

$$\sum_{i=1}^{N} w_i (y_i - \hat{y}_i)^2 \tag{2.1}$$

where y_i represents a measured quantity or target at a time or location indicated by i. $\hat{y}_i$ is the calculated model value which is a function of model parameters or initial conditions. w_i is the weighting function based on some prior information or it can be used to combine different quantities with different magnitude. For measurement errors being proportional to the magnitude of the measurement, large values will be put more weight since the variance is also large. Weighted sum of squares in a relative sense is used as objective function shown in Eq. 2.2.

$$\sum_{i=1}^{N} w_i \left(\frac{y_i - \hat{y}_i}{y_i}\right)^2 \tag{2.2}$$

Based on the most literature, regularization process is regarded as the general procedure to transform the ill-posed problem into a well-posed form [11-13]. There are several different regularization techniques:

- Tikhonov regularization
- Iterative regularization
- Generalized cross-validation
- Kalman filtering approach
- Singular value decomposition

Tikhonov regularization method, developed by Tikhonov [14], was one of the most effective approaches for practical applications, accomplished by adding one or more penalty terms to the objective function, shown in below:

$$\sum_{i=1}^{N} w_i (y_i - \hat{y}_i)^2 + \alpha_0 \sum_{i=1}^{N} f_i \tag{2.3}$$

where α_0 is the regularization parameter that weights the restriction on f_i. The function f_i represents regularization term. Regularization term is chosen so that highly physically meaningful cases will have low restriction, which reduces large-magnitude oscillations.

For the first type of inverse problem, parameter estimation or model calibration, shown in Figure 2.1. Sensitivity analysis and correlation analysis are preferred to apply to determine the design variables for optimization. Sensitivity analysis could be used to evaluate the relative importance of each input parameter. While correlation analysis aims to get rid of correlated parameters since highly correlated parameters optimized simultaneously can lead to the same optimized result with many different combinations, in which unrealistic values of the parameters exist. This will guide the problem to be the ill-posed one.

Another means of sorting is based on the statistical nature of the method employed for solving an inverse problem [12]:

- Deterministic
- Stochastic
- Methods based on artificial intelligence

The typical algorithms for deterministic method are gradient-based algorithms, such as Gauss-Newton algorithm [15] and Quasi-Newton algorithm. Stochastic methods are based on finding statistical relations between input and output. The most useful

statistical model is regression model. Artificial intelligence [16, 17], such as genetic algorithm, fuzzy algorithms and artificial neural networks, is another way to solve an inverse problem.

Studies on different approaches, such as gradient based algorithms and genetic algorithm (GA) [16], solving ill-posed backward inverse problem by Chiwiacowsky et al. [12] have concluded, based on an inverse heat conduction problem, that gradient based algorithms get better results for the case when noiseless data is used and the regularization is not applied. The regularization operator is not necessary to retrieve the initial condition when gradient based algorithms are employed dealing with noiseless data.

There are pros and cons for each methodology according to different applications. Basically, gradient based algorithm usually gets more precise solution and it is much faster for it to be converged. However, the problem should be well defined and assume the solution is unique, since this method always get to the local optimum. On the other hand, method of artificial intelligence is global optimization method, suited for problem with many parameters. Derivative evaluation of the error function is not needed and it is highly efficient in dealing with large, discrete, non-linear and poorly understood optimization problems. But the solution is not accurate and the computational cost is high.

Although application of load identification was analyzed based on the inverse identification method to estimate the contact forces between wheel and rail during rail vehicle operation in the work performed by Uhl [13], inverse analysis techniques have never been applied on a large scale application to identify fatigue damage design loads.

2.2 Cumulative fatigue analysis

Fatigue life for vehicle machine components is typically estimated based on a damage accumulation method, Miner's rule [18]. S-N curve, or stress-life curve, is shown in Figure 2.2, which is used to calculate the number of cycles to fatigue failure ($2N_f$) based on a particular stress amplitude ($\Delta\sigma/2$). For k different stress magnitudes $\Delta\sigma_i$ in a stress history with each contributing n_i cycles, if N_i is the number of cycles to failure of that particular stress range, the total damage is calculated by Miner's rule shown in Eq. 2.4. Fatigue failure occurs when the cumulative damage equals one.

$$D = \sum \frac{n_i}{N_i} \qquad i = 1, 2, \ldots, k \tag{2.4}$$

The fatigue life is the reciprocal of the total damage. It is true that most of the stress (or strain) history data has varying amplitudes in practice. To convert the varying stress history into a series of constant amplitude cycles, the rain flow counting method [19] is generally used to obtain an accurate number of cycles defined as closed stress or strain hysteresis loops.

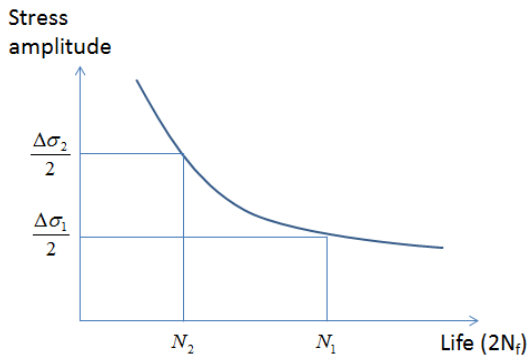

Figure 2.2: Stress amplitude and life curve

Two main approaches are used to obtain the stress or strain history data for the damage estimation; transient dynamic analysis methods [20, 21] and quasi-static stress analysis methods [22]. Transient dynamic analysis methods deal with high inertial structural system with large vibrational effects. Quasi-static stress methods, on the other hand, are used for structural system with less inertia effects and external loads applied below the system natural frequency, which can get accurate enough approximate stress history for a concept design evaluation. Hence, in this study, the stress or strain history of a vehicle machine is generated by the quasi-static stress analysis methods. Firstly, a linear elastic finite element analysis is performed by applying static unit loads at the degrees of freedom where individual load histories are applied. Then, based on the load histories of each degree of freedom, the resulting unit load stress responses, or static stress influence coefficients, will be scaled. Finally, a complete stress history for the damage accumulation is obtained by combining all the scaled unit load stresses at each loading time point sequentially. For cases with multi-axial stress status, it is not intuitive which plane direction will have the most severe fatigue damage since the phase relationship between the stress components is not constant. The critical plane method [23] projects the stresses onto several planes and fatigue damage at each plane is calculated. The most severe plane for fatigue damage is interpolated with the calculated planes. For comprehensive details on the multi-axial fatigue life analysis, the reader is referred to any classical method [23-25].

2.3 Taguchi design

Enough relevant data are always good for researchers to infer the science behind the observed phenomenon. The typical way to achieve the goal is trial-and-error approach.

A series of experiments are performed to get some understanding. However, the data is insufficient to draw any significant conclusions because of the lack of logic performing experiments. A well planned set of experiments, in which all parameters of interest are varied over a specified range, is a much better approach to obtain systematic data. The concept of design of experiments was introduced by Fisher in the early 1920s [29]. Taguchi went further with the design of experiment concept by introducing his approach in 1986 [30]. Taguchi design is one of the approaches to reduce variance for the experiment with optimum settings of control parameters. The combination of design of experiments with optimization of control parameters to obtain best results is achieved in the Taguchi design.

The Taguchi design is an efficient and effective robust design of experiments method in which a response variable can be optimized to reduce the variation of this process, given various control and noise factors, using fewer resources than a factorial design. The overall objective of Taguchi design is to produce high quality product at low cost to the manufacturer, developed by a Japanese engineer Dr. Genichi Taguchi. The application had been widespread in many US and European industries after 1980s. The general steps involved in the Taguchi Method are as follows in Figure 2.3:

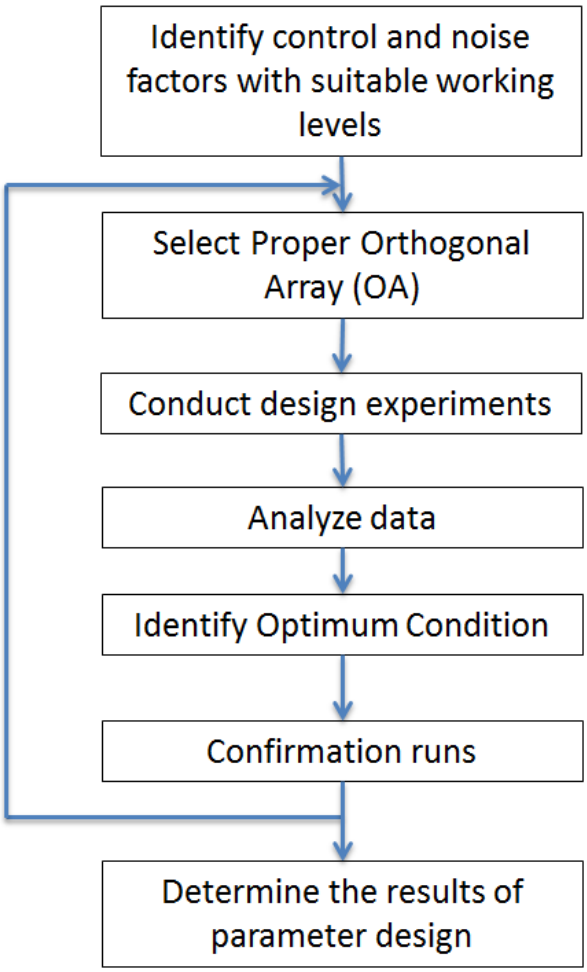

Figure 2.3: Schematic of Taguchi design

The most important part of Taguchi design is the parameter design, in which multiple factors can be considered, including control factors and noise factors. Control factors are variables under management control, while noise factors come from uncontrollable variation. Also, levels of control and noise factors should be determined. Opposite to full factorial analysis, the Taguchi Design reduces the number of experimental runs to a reasonable one, in terms of cost and time by using Orthogonal Arrays [31]. Choosing the proper Orthogonal Array suitable for the problem of interest is the main difficulty of Taguchi Design [30]. Table 2.1 shows an example of L9 Array with

3 levels of each parameter. Orthogonal Array (OA) is chosen based on the number of control factors, which makes this process even more effective than a fractional factorial design. There are different experiment objectives represented by three signal-to-noise ratios shown below in Eq. 2.5, 2.6, 2.7, which measures how the response varies relative to the nominal or target value under different noise conditions.

- Smaller-the-better

$$S/N = -10 \times \log(\frac{1}{n}\sum \hat{Y}_i^2) \tag{2.5}$$

- Larger-the-better

$$S/N = -10 \times \log(\frac{1}{n}\sum \frac{1}{\hat{Y}_i^2}) \tag{2.6}$$

- Nominal-the-best

$$S/N = 10 \times \log(\frac{\overline{Y}^2}{\sigma^2}) \tag{2.7}$$

Here, n is the number of observations on the particular product, and Y is the respective characteristic. The second case can be converted to the first case by taking the reciprocals of the measured data. Smaller-the-better try to minimize the response and large-the-better maximize the response. Smaller-the-better is used for the ideal value with all undesirable characteristics zero or the ideal value is finite and its maximum or minimum value is defined. As for nominal-the-best, a specified value is most desired and neither a smaller nor a larger value is desirable in this case. Data analytics are performed

according to the experimental objectives before a confirmation run. Typically, this process is an iterative manual process.

Table 2.1: L9 Orthogonal Array with 3 levels of each factor

Experimental Runs	Factor (Levels)			
	A (3)	B (3)	C (3)	D (3)
1	1	1	1	1
2	1	2	2	2
3	1	3	3	3
4	2	1	2	3
5	2	2	3	1
6	2	3	1	2
7	3	1	3	2
8	3	2	1	3
9	3	3	2	1

3. Proposed methodology

This chapter introduces the methodologies proposed for fatigue design load development and automatic Taguchi Design. There are two processes for fatigue design load development which is shown in Section 3.1 and 3.2. Section 3.3 introduces the framework for automatic Taguchi Design.

The proposed Engineering Data Analytics (EDA) approach integrating data analytics and physics-based engineering mechanics has to processes shown in Figure 3.2. Process I is for fundamental fatigue load pattern identification and fatigue design load transformation is in Process II.

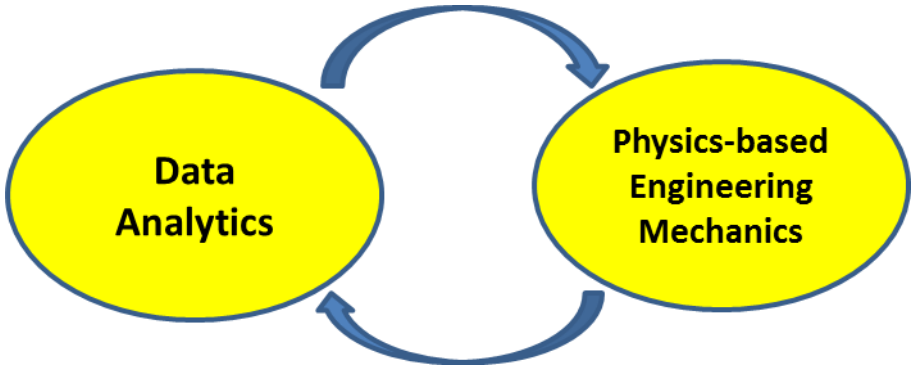

Figure 3.1: Conceptual ideal for fatigue design load development

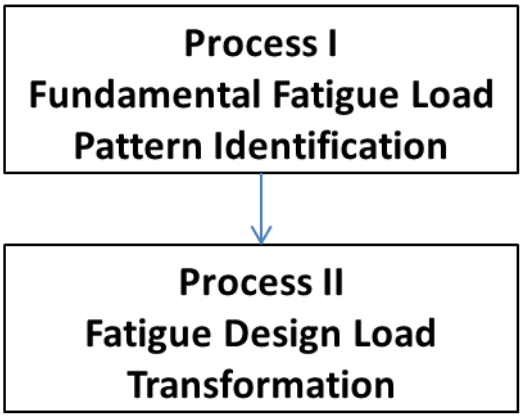

Figure 3.2: Two processes for fatigue design load development

3.1 Fatigue load pattern identification using Engineering Data Analytics (EDA)

Data analytics is a general knowledge discovery process to obtain better understanding and new information out of huge amounts of data [10, 26, 27]. In data analytics, a broad range of techniques are used, such as data acquisition and selection, data cleaning and screening, data transformation, interpretation and feature modeling, and prediction. In this study, the EDA approach [10] is used to find the fundamental fatigue load patterns based on data transformation, pattern mining, and data featuring techniques. In the EDA method, first, instead of working on the measured loads directly, the engineering fatigue mechanics is incorporated to transform and characterize the data in terms of the fatigue damage. Fatigue based sensitivity is also utilized to highlight hidden damage patterns within the large amounts of load data. By using data pattern mining, critical load patterns of fatigue damage are identified among all the observation locations. The process of the fatigue load pattern identification via Engineering Data Analytics (EDA) is presented in Figure 3.3. The following subsections show detail steps of the EDA method.

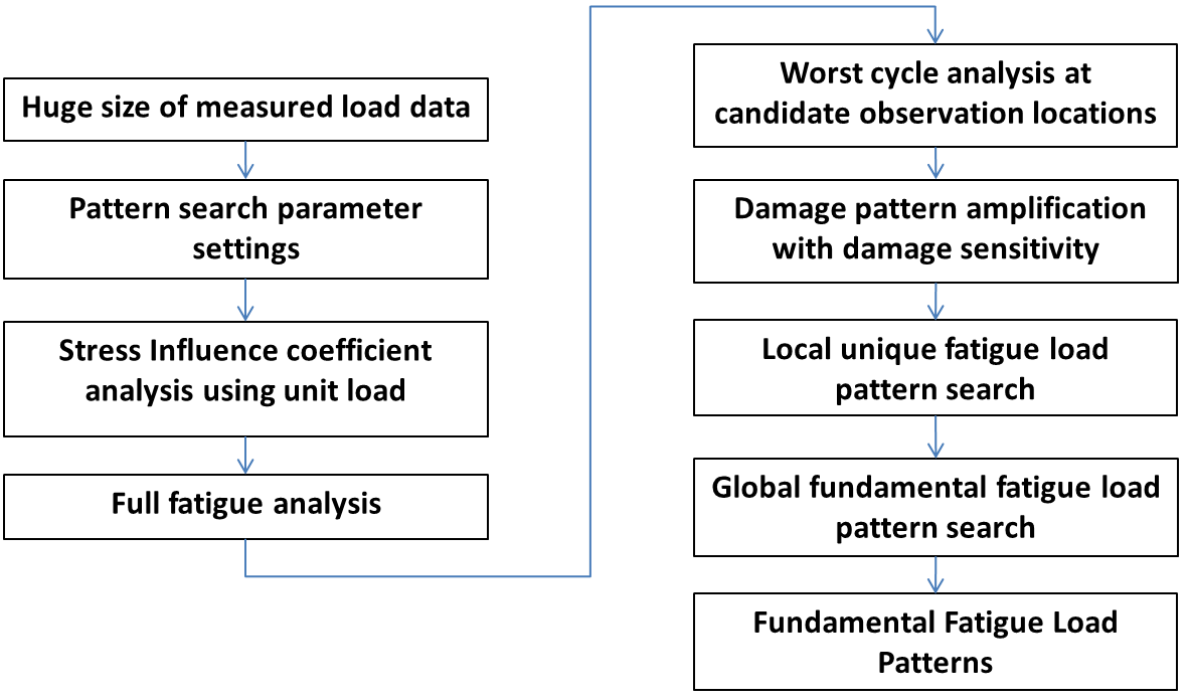

Figure 3.3: Process I: EDA based fatigue load pattern identification

3.1.1 Full life analysis and worst cycle fatigue loads

Assuming a Finite Element (FE) model is available for the quasi-static stress analysis, the unit load analysis is performed to obtain the stress influence data by applying unit loads at the degrees of freedom where individual load histories are applied. Then, the full stress history at a location of interest is recovered by multiplying load history data to the stress influence data as in the following equations.

$$\sigma_j = \sum_i L_{ij} U_i \qquad i = 1,2,...,I \;\; j = 1,2,...,J \tag{3.1}$$

$$U_i = \{U_{xx\_i} \; U_{yy\_i} \; U_{xy\_i}\}^T \tag{3.2}$$

$$\sigma_j = \{\sigma_{xx\_j} \; \sigma_{yy\_j} \; \sigma_{xy\_j}\}^T \tag{3.3}$$

Here, I is the total number of loading locations, J is the total number of load history time points, L_{ij} is a load component on the i^{th} loading location at the j^{th} time point in the load history data, U_i is the stress influence coefficient data obtained by applying a unit load at the i^{th} loading location consisting of three influence coefficients U_{xx_i}, U_{yy_i} and U_{xy_i} for the plane stress, and σ_j is the stress status at the j^{th} time point at a location of interest also consisting of three plan stress components σ_{xx_j}, σ_{yy_j} and σ_{xy_j}. In practice, there are many different fatigue life assessment algorithms depending on load types (high or low cycles), materials, temperature, or residual stress and manufacturing methods such as a casting or fabricated structure. In this study, the main purpose of performing the full life analysis is to examine the load data by transforming it into cyclic loads. Therefore, the multi-axial principal stress algorithm with no mean stress correction is selected for a conservative life assessment of a general fabricated structure.

Once the fatigue analysis is performed, damage information can be extracted from the recovered full stress history in terms of the critical damage plane, worst cycles, and their frequencies. The number of worst cycles depends on the ratio of the total fatigue damage to be covered and the complexity of the load history data. For example, the 90% coverage ratio of the total fatigue life would include more worst cycles than the 80% coverage ratio. In practical cases, the number of extracted worst cycles can be controlled by segmenting the measured load data based on unique types of dynamic events. This worst cycle information in Eq. 3.5 is the transformed load data that will be used for the rest of the EDA process.

$$L_j = \{L_{ij} \mid \forall i\} \tag{3.4}$$

$$FL_k = (L_{wc_{2k}} - L_{wc_{1k}}) \quad k = 1, ..., K_e \tag{3.5}$$

Here, L_j is the load vector given at the j^{th} time point in a load history data, wc_{1k} and wc_{2k} are the load history time points for the k^{th} worst cycle, K_e is the total number of identified worst cycles at the location of interest, and FL_k is the k^{th} worst cycle fatigue load vector. As a result, for multiple locations of interest on a target structure, a matrix of worst cycle fatigue load vectors, FL, is obtained by

$$FL = \{FL_{kp} \mid k = 1, 2, ..., K_e; p = 1, 2, ..., P\} \tag{3.6}$$

where P is the total number of observation locations.

The next step is to find basic patterns among the fatigue load vectors in FL. In practice, typically the size of the FL matrix is computationally challenging to deal with altogether within a single EDA process. In the EDA method, to take advantage of parallel computing power, the pattern mining is divided into two stages, local and global pattern mining. The local pattern mining is performed at individual observation locations, and later fundamental fatigue load patterns are obtained among the local ones through the global pattern mining. The local pattern identifications can be distributed to multiple processors to reduce the computational time since the interaction effects among the basic patterns are addressed by the global pattern mining. In the pattern mining, it should be considered that the same load patterns can be found in multiple locations, and a load pattern which is insignificant at one location could be highly damaging at other locations. Depending on the structural configurations and locations, the sensitivities of load patterns

to fatigue damage could vary. Hence the sensitivity needs to be incorporated along with the pattern mining.

3.1.2 Pattern amplification using damage based sensitivity in EDA

Before pattern mining, the fatigue load vectors are weighted with damage based sensitivities to amplify hidden patterns in terms of fatigue damage according to the location they belong. The fatigue damage at a location is a function of stress ranges along the critical plane direction obtained from the previous full fatigue analysis. At a given critical plane direction (θ_c) for the j^{th} load history point, the stress is obtained as

$$\sigma_{x1\_j} = \frac{\sigma_{xx\_j} + \sigma_{yy\_j}}{2} + \frac{\sigma_{xx\_j} - \sigma_{yy\_j}}{2}\cos 2\theta_c + \sigma_{xy\_j}\sin 2\theta_c \tag{3.7}$$

where the plane stress components, σ_{xx_j}, σ_{yy_j}, and σ_{xy_j}, are from Eq. 3.1-3.3. The damage based sensitivity is approximated by the stress sensitivity which will be unique at each observation location as

$$\frac{\partial \sigma_{x1}}{\partial L_i} = U_{xx\_i}(1+\cos 2\theta_c)/2 + U_{yy\_i}(1-\cos 2\theta_c)/2 + U_{xy\_i}\sin 2\theta_c \tag{3.8}$$

where U_{xx_i}, U_{yy_i} and U_{xy_i} are the three stress influence coefficients from the unit load stress analysis. The sensitivity vector which approximates the damage sensitivity is obtained by Eq. 3.9 at each observation location p. Then the matrix of pattern-amplified fatigue load vectors (wFL_{kp}) are obtained in Eq. 3.10, which is essentially scaled by the damage based sensitivity (DS_p) for each fatigue load vector k at each location p.

$$DS_p = \left\{ \left. \frac{\partial \sigma_{x1}}{\partial L_i} \right|_p ; i = 1, 2, ..., I \right\} \qquad p = 1, 2, ..., P \tag{3.9}$$

$$wFL_{kp} = DS_p .* FL_{kp} \tag{3.10}$$

here, the operator (.*) is for the component wise multiplications of two vectors.

3.1.3 Local and global basic pattern identifications

The EDA method employs two stages – the local and global mining processes of the fundamental fatigue load patterns. Again, the goal in this study is to capture all the fundamental fatigue load patterns by the measured data. Therefore, identifying all the fundamental load patterns is the key task. Once the fundamental fatigue load patterns are identified, they can be used to determine the fatigue design loads for conceptual design.

First, the local pattern mining is performed at each observation location. The pattern-amplified fatigue load vectors (wFL_k) at an observation location are cross-compared to each other to obtain a Normal Vector Correlation (NVC) which is defined by

$$NVC_{mn} = \frac{\left| wFL_m^T \cdot wFL_n \right|^2}{wFL_m{}^T wFL_m wFL_n{}^T wFL_n} \qquad m = 1, ..., K_e,\ n = 1, ..., K_e \tag{3.11}$$

where K_e is the total number of amplified fatigue load vectors at an observation location of interest and the superscript T indicates the transposition of the vector. The NVC measurement is essentially the same as the Modal Assurance Criterion (MAC) [29] which is a common measure to estimate the correlation among the modal shapes in SHM. NVC measures the degree of correlation between two fatigue load vectors. In the local process,

any fatigue load vector that has the NVC values to all other vectors lower than a correlation threshold (corr_tol) is regarded as a unique load pattern and kept in the LFL_u as in Eq. 3.12. But on the other hand, if any vector shows high NVC, it will be taken as a dependent load pattern and excluded from wFL. This local pattern mining will eliminate correlated load patterns sequentially in the order of fatigue damage severity. In Eq. 3.12, lK_e starts with K_e and updates itself as high NVC load vectors are excluded in a sequential process.

$$LFL_u = \{wFL_m \mid \forall NVC_{mn} < corr\_tol \;\; ; n = m+1, ..., lK_e; m = 1, 2, ..., lK_e\} \tag{3.12}$$

At the end of the local pattern mining with a given correlation threshold, only uncorrelated patterns are stored in LFL_u as locally-unique fatigue loads for the current observation location p. The correlation threshold is a user defined control parameter for the pattern mining. It is expected the higher the correlation threshold, the larger the number of unique fatigue load vectors. This local process is repeated for all observation locations and the full matrix of locally-unique fatigue load vectors (LFL) is obtained as

$$LFL = \{LFL_{up} \mid u = 1, 2, ..., U_p; p = 1, 2, ..., P\} \tag{3.13}$$

where U_p is the total number of unique fatigue loads at the observation location p. Typically the size of LFL (Eq. 3.13) becomes much smaller than FL (Eq. 3.6) as only unique pattern fatigue loads are collected from each observation location.

Next, the global mining process is performed to identify fundamental fatigue loads for the entire structure from LFL. For the global process, the LFL fatigue load

patterns from each observation location are rearranged into the LFLV vector as in Eq. 3.14 where C is the total number of the load patterns from all the observation locations.

$$\begin{aligned} LFLV &= \{LFL_{u1}^{T}, LFL_{u2}^{T}, \cdots, LFL_{up}^{T}\} \\ &= \{LFLV_c \mid c = 1, 2, ..., C\} \end{aligned} \tag{3.14}$$

In the global process, the NVC measurements for the LFLV vectors are again compared to each other to find fundamentally unique fatigue load patterns through the entire observation locations. However, unlike the local mining, the global process needs to consider a global NVC matrix which consists of multiple sets of the NVC values obtained by applying different damage based sensitivity amplifications of each observation location as

$$gNVC_{c_1c_2|p} = \frac{\left| wLFLV_{c_1|p}^{T} \cdot wLFLV_{c_2|p} \right|^2}{wLFLV_{c_1|p}{}^{T} wLFLV_{c_1|p} wLFLV_{c_2|p}{}^{T} wLFLV_{c_2|p}}$$

$$c_1 = 1, ..., C,\ c_2 = 1, ..., C,\ p = 1, ..., P \tag{3.15}$$

where

$$wLFLV_{c_1|p} = DS_p .* LFLV_{c_1}$$

The global NVC matrix starts with all LFLV load vectors in the beginning of the global process. However, if a pair of LFLVs shows higher values than the user defined correlation threshold at all the observation locations, they are taken as the same load pattern. The process is performed sequentially in the order of structural damage contribution until only fundamental fatigue load (FFL) vectors are left (Eq. 3.16).

$$FFL_q = \{LFLV_{c_1} \mid \forall(\min[gNVC_{c_1c_2|p}, p = 1, 2, \ldots, P]) < corr\_tol\ ; c_2 = c_1 + 1, ..., lC; c_1 = 1, 2, ..., lC\} \quad (3.16)$$

here, lC starts with the total number of LFLV and updated itself sequentially as correlated LFLV vectors are removed from gNVC. As a result of the global mining process, the patterns of FFLs are obtained by

$$FFL = \{FFL_q \mid q = 1, 2, ..., Q\} \quad (3.17)$$

where Q is the total number of FFL patterns. In most practical cases, the size of FFL is significantly smaller than the originally measured load data. The process also keeps the association information (Eq. 3.18) of the LFLV to the individual fundamental fatigue load patterns which are used in the next step to determine the fatigue design loads.

$$FFL_q = \{LFLV_q \lhd LFLV_h\ h = 1, 2, ..., H_q\} \quad (3.18)$$

here, H_q is the number of correlated local fatigue load vectors for the q^{th} fundamental fatigue load pattern.

3.2 Fatigue design load transformation via two-stage optimizations

The patterns in FFLs obtained from the previous step are not actual loads, but they represent fundamental patterns for the fatigue damage from the measured load data. They are unique to each other, representing different aspects of the full loading. As mentioned before, the FFL patterns need to be converted to the applicable static fatigue design loads using engineering optimization techniques, which will be addressed by Process II shown in Figure 3.4 In the proposed method, the scale and frequency of each

FFL pattern are considered as the main factors since applying different scales and number of repeats of the FFL patterns leads to variation of the severity and distribution of the fatigue damage to the structure. Block loading for each FFL, instead of putting all FFL patterns within one block, is used as the manner to apply fatigue design load in order to get rid of sequence and transition effects. Thus, the scale and frequency for each fundamental fatigue load pattern are determined as the design variables for the optimization in the fatigue load transformation. The goal of the optimization is to obtain the fatigue design loads which give rise to the exact match of the fatigue damage compared to the results from the full set of loading history across the target structure. The proposed two-stage optimizations to determine the scales and frequencies for each fatigue load pattern is shown as in Figure 3.5.

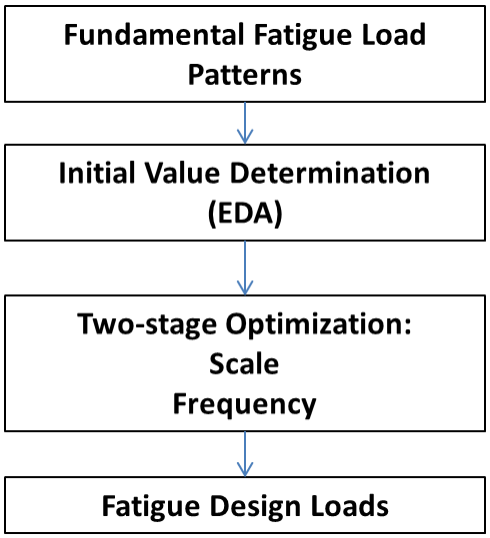

Figure 3.4: Process II: fatigue design load transformation

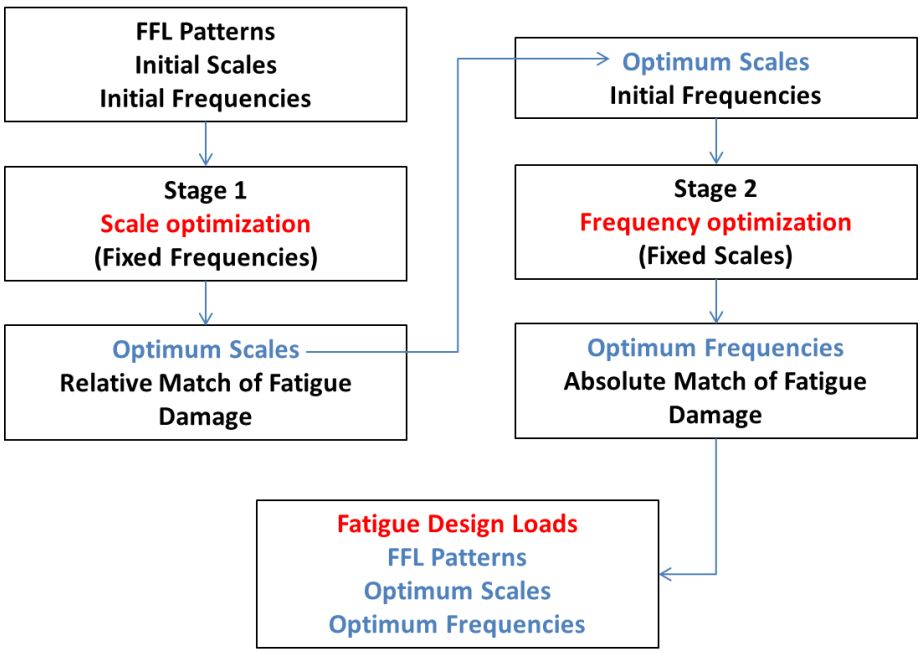

Figure 3.5: Two-stage optimizations

Before performing the two stages of optimizations, the initial values for design variables are determined by using EDA again in order to get rid of odd cases for the design loads. Based on the association information obtained from local and global basic pattern identifications, all correlated local fatigue loads corresponding to each fundamental fatigue load pattern in FFLs (Eq. 3.16) are extracted for the process of EDA. There could be some local fatigue load vectors that are captured in multiple observation locations. In that case, the duplicated loads will be eliminated based on the association information, in which the load history time points are compared one by one. By applying the EDA techniques to get the distribution for all load patterns in FFLs, initial scales are determined using median values. Initial frequencies are achieved solving optimization problems (Eq. 3.19) for each FFL pattern to get approximated fatigue damage match with

respect to the damage caused by all correlated local fatigue load vectors. A flowchart of this process is shown in Figgure 3.6.

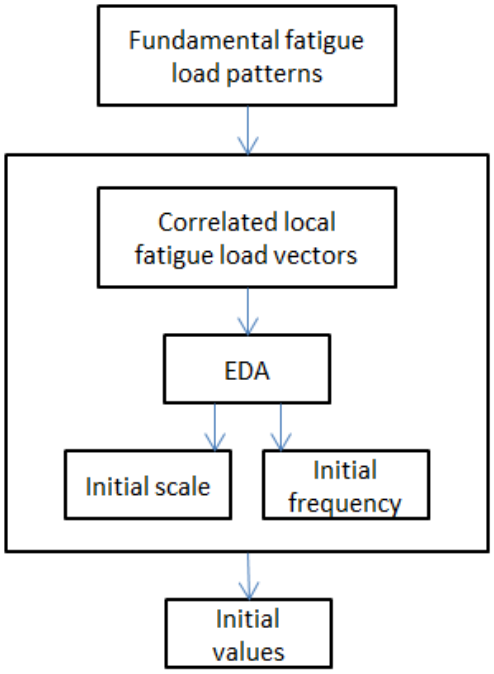

Figure 3.6: Process for initial values determination

$$Minimize: \sum_{p=1}^{P} w_p \left[d_p(f_q) - d_p^t \right]^2$$

$$Subject\ to: \ f_{lb} < f_q < f_{ub} \tag{3.19}$$

where p is the number of virtual gage locations. q is the number of fatigue design loads. $d_p(f_q)$ is fatigue damage applying qth fundamental fatigue load pattern with frequency f_q at location p. d_p^t is the targeted fatigue damage from all correlated local fatigue load vectors at location p. f_{lb} and f_{ub} are the lower and upper bounds of frequencies. w_p is the weighting function assigned by user based on the prior information.

After getting the initial guess of the scales and frequencies for each FFL pattern, two-stage optimizations are performed: scale and frequency optimizations. As shown in Figure 3.5, in the first stage of the scale optimization, fatigue damages caused by the full sets of the load history and the fundamental fatigue design loads are matched up in a relative sense at all the observation locations while the frequencies are fixed. This is achieved by calculating the relative damage according to a reference location and using a single objective function formed by combining normalized fatigue damage of all the observation locations. Scale optimization formulations are defined as Eq. 3.20.

$$\begin{aligned} &Minimize: \sum_{p=1}^{P} w_p\left[d'_p(\boldsymbol{S}) - d'^t_p\right]^2 \\ &Subject\ to: S_{lb} < \boldsymbol{S} < S_{ub}, \boldsymbol{S} = [S_1, S_2, \dots, S_q] \end{aligned} \tag{3.20}$$

where p is the number of virtual gage locations. q is the number of fatigue design loads. $d'_p(\boldsymbol{S})$ and d'^t_p are the normalized fatigue damage from fatigue design loads with scales $\boldsymbol{S}$ and full loading history for location p, respectively. $\boldsymbol{S}$ represents the scales of all fatigue design loads. S_{lb} and S_{ub} are lower and upper bounds of scales. w_p is the weighting function assigned by the user based on the prior information.

The purpose of having two-stage optimizations is that the imrelative match of the fatigue damage contour is expected in the scale optimization, while the absolute damage values will be addressed in the second stage of optimization by adjusting the frequencies. Frequency optimization is performed in a similar way as the previous approach. The scales obtained from the first stage are fixed and frequencies are the design variables. The difference is that the absolute match of the fatigue damage is addressed by combining the relative error with respect to the targeted fatigue damage for all the observation locations

in the objective function. After frequency optimization, the fundamental fatigue design loads with optimum scales and frequencies will produce the same magnitudes of fatigue damage as the full loading for all the observation locations. Frequency optimization is described by Eq. 3.21.

$$\begin{aligned} Minimize: & \sum_{p=1}^{P} w_p \left[\frac{d_p(f) - d_p^t}{d_p^t}\right]^2 \\ Subject\ to: & \ f_{lb} < f < f_{ub}, f = [f_1, f_2, \dots, f_q] \end{aligned} \tag{3.21}$$

where p is the number of virtual gage locations. q is the number of fatigue design loads. d_p and d_p^t are the absolute fatigue damage from fatigue design loads and full loading history. $\boldsymbol{f}$ represents the frequencies of all fatigue design loads. f_{lb} and f_{ub} are lower and upper bounds of frequencies. w_p is the weighting function assigned by the user based on the prior information.

In this study, two stages of optimizations are adopted to find a small set of fundamental fatigue design loads which can replace the full loading history with the same damage on the structure. In a practical application, there would be additional considerations such as the number of virtual gage locations to choose and the computational time to perform this process. For those challenges and complexities in the fundamental load identification, the numerical optimization strategies would come into picture.

3.3 Automatic Taguchi optimization toolkit

This section shows the basic idea to achieve the automatic process for Taguchi design through engineering data analytics, regression analysis and optimization

techniques. This process has been coded in a toolkit using programing language Python. The DAKOTA (Design Analysis Kit for Optimization and Terascale Applications) from Sandia National Laboratories, a multilevel parallel object-oriented framework, is used as optimization tool.

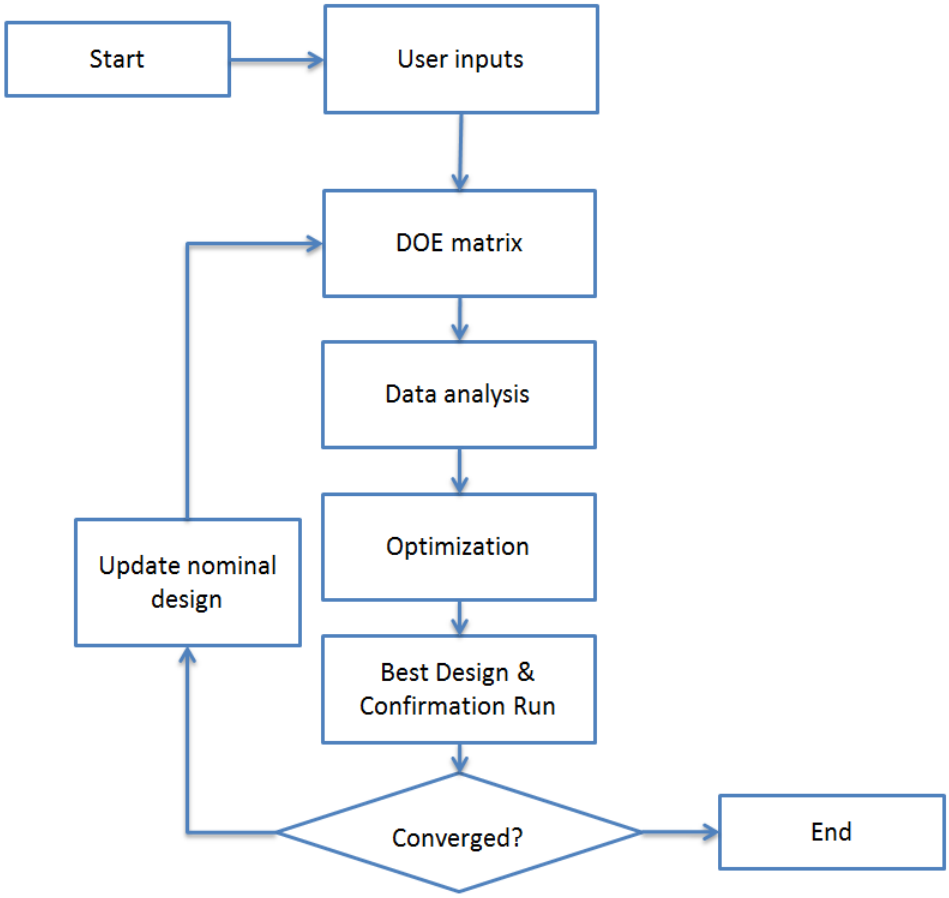

Figure 3.7: Overall process of automatic Taguchi optimization

The overall flowchart of this automatic process is shown in Figure 3.7. Based on the user's inputs assigned in the beginning of the process, design of experiments (DOE) is performed based on the Orthogonal Array (OA) assigned by the user. Data analysis is performed to calculate the corresponding SN ratio according to the experiment objective.

Then, regression model is built according to the data analytics results. In order to get the robustness design, an optimization problem is set up. After getting the optimum results, confirmation run is performed. This is an iterative process and it will stop till the convergence criteria meets. Detail of each part will be discussed in the following parts.

For user's inputs, it basically defines the problem and how to solve the problem. The following aspects will be assigned in this stage by the user:

- Control/ Noise Factors
- Responses
- Orthogonal Array
- Regression Model Type
- Termination Criteria
- Dakota Optimization
- Other related parameters

For control and noise factors, several parameters are defined, such as lower and upper bounds, number of levels for DOE, starting points of control factors and descriptors. Besides, if there are multiple responses, weight for each response will be assigned as well. The Orthogonal Array is given directly by user. Regression Model will be used during this process and the user has the feasibility to choose different type of it. Termination Criteria is defined through the termination tolerance assigned by the user. Some parameters to control the optimization for Dakota toolkit are also assigned in this process, such as the maximum iteration, local range ratio, convergence tolerance and etc. Other related parameters will be explained in the following part.

DOE is performed based on the selected Orthogonal Array and starting points within a local range. This specific local range is defined by the local range ratio in a form of percentage out of the whole design domain. This local range will be updated in the following process based on some criteria. Which Orthogonal Array to choose depends on the how many number of levels control factors have. Determining what levels of a variable to test requires an in-depth understanding of the process, including the minimum, maximum, and current value of the parameter. If the range of a parameter is large, more levels can be defined for Taguchi design. If the range is narrow, fewer levels can be chosen or the values to be tested can be closer together.

After the process of design of experiments, a DOE matrix, in which all responses are calculated according to corresponding control and noise factors, is built up for the data analytics if there is only on responses. For case with multiple responses, multiple DOE matrixes are calculated. The number of DOE matrixes is the same as the number of responses. In DOE matrix, each row represents that particular response in the case with control factors fixed and the noise factors are kept changing. Each column represents the responses with fixed noise factors and changing control factors. Then mean values and standard deviations of each row, which means control factors are fixed, for each response, are calculated. Based on the goal of this experiment, signal-to-noise values are calculated for each case based on the responses, mean value and standard deviation. The SN values and the control factors will be used for regression analysis. Linear least square regression models for responses or SN values will be built based on the control factors and mean of responses or SN values. Based on the user's inputs, interaction effects of least square models can be chosen to be included or not. Eq. 3.22 and 3.23 represent the SN ratio and

mean value least square for one response. Least square model building with mean of responses represents the tendency of that particular response. SN value least square model indicates the trend of robustness of the system as the control factors go up or down. Typical Taguchi manual process will create the SN ratio effects plot and response effects plot. Based on these two types of plot along with individual experience, new design point will be determined, which is difficult for young engineers without much expertise. Thus, optimization techniques will be applied to achieve an automatic process instead of manual process to determine the new design points for next design iteration.

$$Y_{SN} = b_0 + b_1 x_1 + b_2 x_2 + \cdots + b_n x_n \tag{3.22}$$

$$Y_{Mean} = c_0 + c_1 x_1 + c_2 x_2 + \cdots + c_n x_n \tag{3.23}$$

Our goal is to get the design that meets the requirements, such as equality or inequality constraints for the responses, with the most robust design, which means maximization of the SN ratio. There are several cases for setting up the optimization formulas. Eq. 3.24 is the objective function. Equality or inequality constraints can be added as the constraints for different problems.

$$\text{Minimize: } \sum_{i=1}^{N} w_{SNi} \times (-Y_{SNi})$$

$$\text{Subject to: } \boldsymbol{lb} < \boldsymbol{x} < \boldsymbol{ub} \tag{3.24}$$

Based on the least square model within the local range, the optimum points for the control factors are determined by the optimizer. Whether to update the local range or make it smaller to do design of experiments for next iteration depends on the location of

optimum points since performing design of experiments within a small range will increase the accuracy to capture the local feature by least square model.

- Scheme 01: update local range ratio when the optimum point is inside the range applying the edge percentage

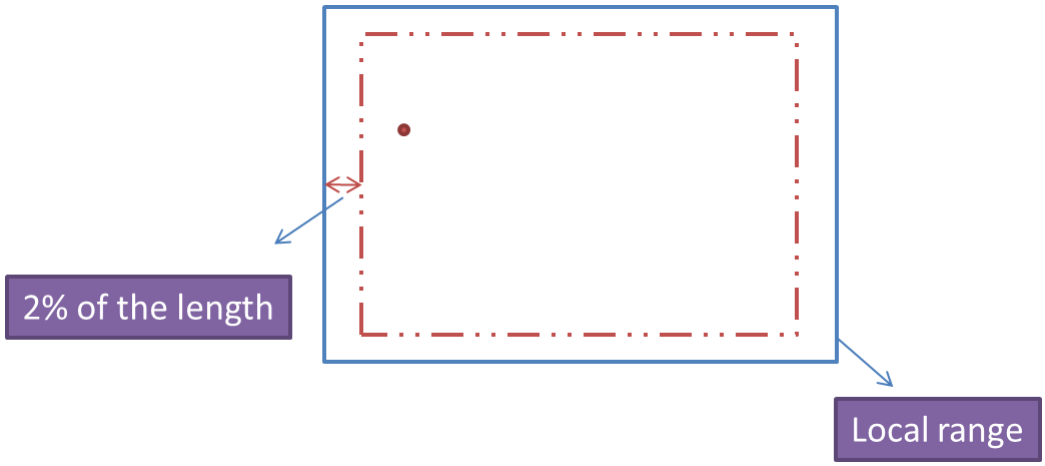

Figure 3.8: Criteria for updating local range ratio (Scheme 01)

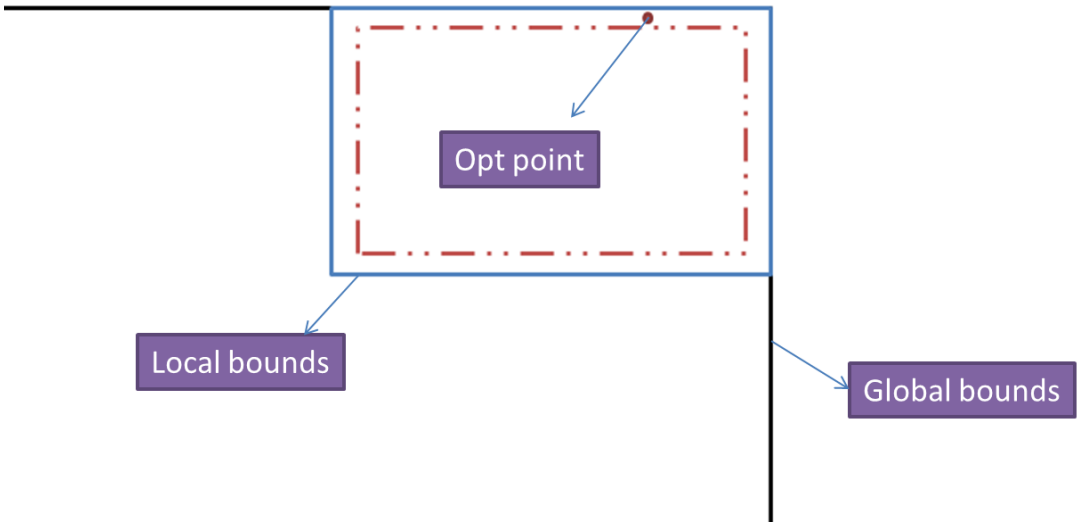

Figure 3.9: Criteria for updating local range ratio (Scheme 02)

- Scheme 02: update local range ratio if the optimum point hits both local and global bounds at the same time

There is a new window defined for checking the criteria of updating local range, denoted as red dot line shown in Figure 3.8 and 3.9. This new window is controlled by the edge percentage for updating local range, which can be adjusted by the user. In another word, this new window is squeezed based on the local range by 2% in length and height for both sides in the example shown in Figure 3.8. The red dot indicates the optimum point from last iteration. If the optimum point is within the newly defined window shown in Figure 3.8, which means the final optimum point is not far away from this local range, the local range ratio will be scaled with local range update ratio. The local range will become smaller in the next iteration. If the optimum point is between the newly defined window and local range, the process will consider that the final optimization point is still far away; the local range will keep moving but not become smaller.

For Scheme 02 shown in Figure 3.9, which is a special case because the optimum point is located between these two windows. According to Scheme 01, local range will not be updated. However, based on the global range for control factors, the optimum point cannot go out of the global range. By doing design of experiments without updating the local range, oscillation will happen. Thus, the local range will keep updating in this case till it focuses the final optimum point. Figure 3.10 shows an example for the case with two control factors. The optimum point hits the local bounds for the first three iterations. The local range keeps moving without becoming smaller until the optimum

point hits the global bounds where Scheme 02 applies. Finally, the local range keeps updating till the final optimization results be focused.

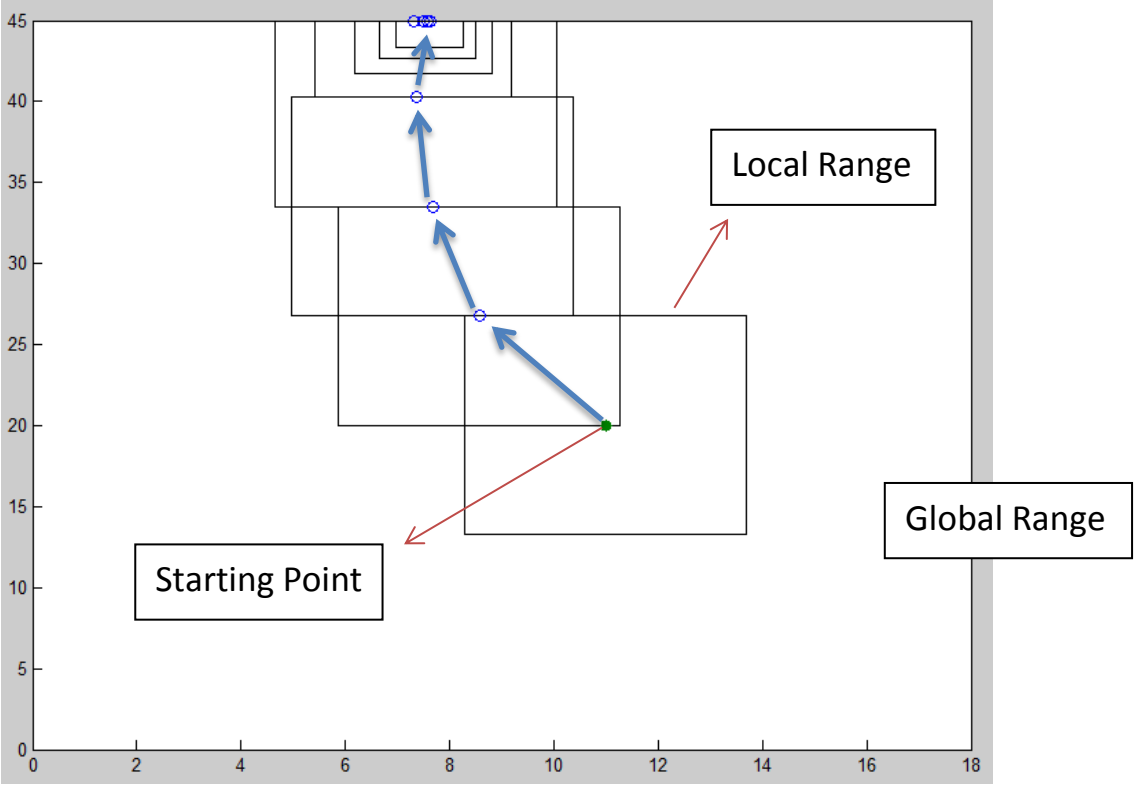

Figure 3.10: Local range updating example

DOE matrix is built as the same way explained before based on the same Orthogonal Array after the local range updating check. Figure 3.11 shows the convergence criteria for the Taguchi design. The basic idea is that either control factors or functions are converged, stop the iteration. Control factors are converged means all the control factors are converged. So are the functions. There are two termination ratios in the user's inputs, one is for control factors, and the other one is for objective functions and constraints. This iterative process will terminate till the convergence criteria meets. This process successfully transfers the usual manual work to the automatic way.

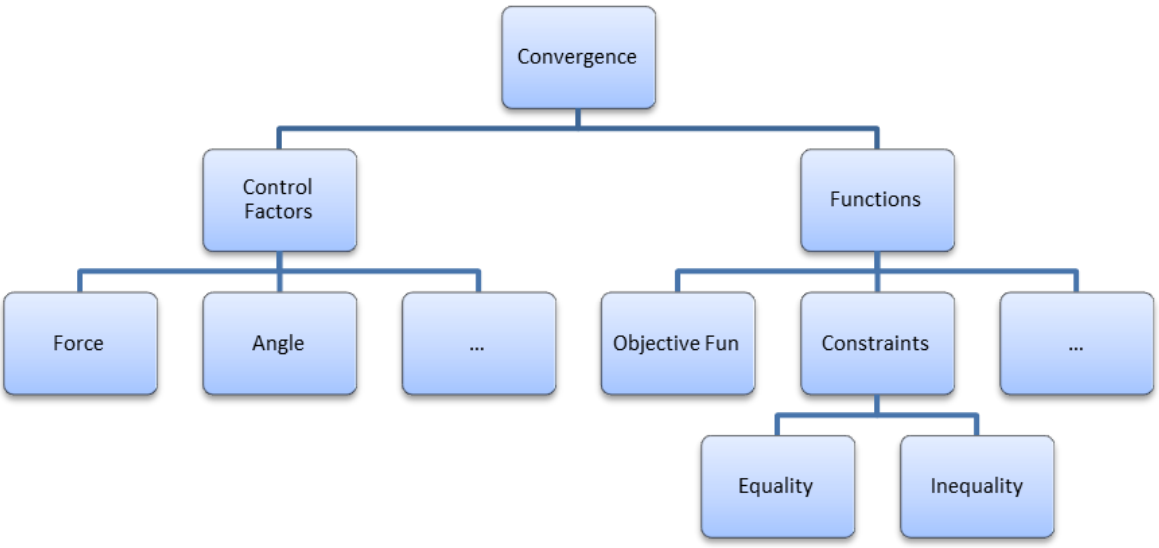

Figure 3.11: Convergence criteria for Taguchi design

4. Numerical demonstrations

In this chapter, two numerical examples are introduced to demonstrate the EDA method to identify fatigue design loads, a common structural component, I-section cantilever beam and an industrial scale front linkage structure, boom. Then Taguchi Design toolkit applying on a simple uniform cantilever beam is used to demonstrate this method.

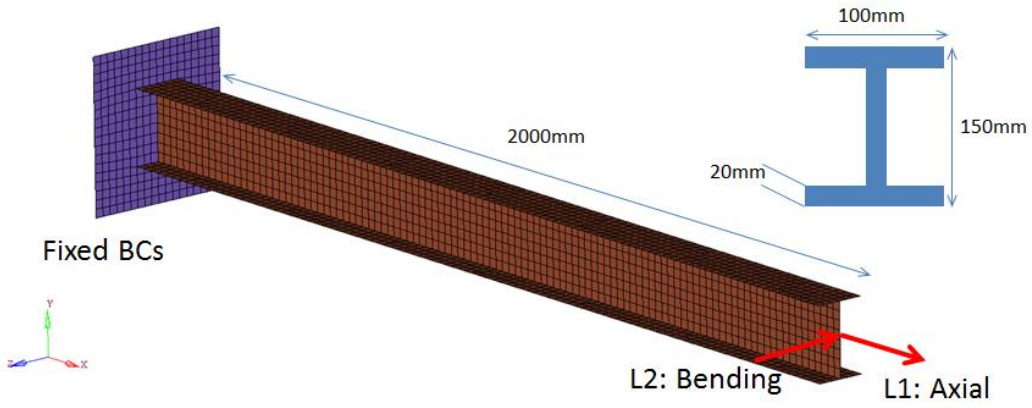

Figure 4.1: I-section cantilever beam

4.1 Fatigue design load development

4.1.1 I-section cantilever beam

The cantilever beam described by Figure 4.1 is used as a numerical demonstration of the proposed method. The cantilever beam has the I-type cross section. With one end fixed, the other free side has two loading inputs; bending and axial. Material properties are assumed to be the typical steel properties of $E=205000N/mm^2$ and $\nu=0.3$. As described in the previous section, unit load stress analysis is performed to obtain the

stress influence coefficient data as shown in Figure 4.2. It is clearly shown the bending stress (unit: MPa) is higher than the axial stress with the unit loads. Load history data which has a limited number of cyclic fatigue loads for the demonstration is shown in Figure 4.3. From the load history data, the fatigue damage from the repetitive segment is expected to occur. The fatigue analysis is performed by using the commercial fatigue life analysis code Fe-Safe [28]. As discussed in the Section III, the linear damage fatigue analysis with quasi-static stress history is performed with the maximum principal stress algorithm and the SN curve for ISO steel 1020 from the material database built into Fe-safe. The fatigue life contour over the cantilever beam is shown in Figure 4.4 in terms of the repetitions of the given load history.

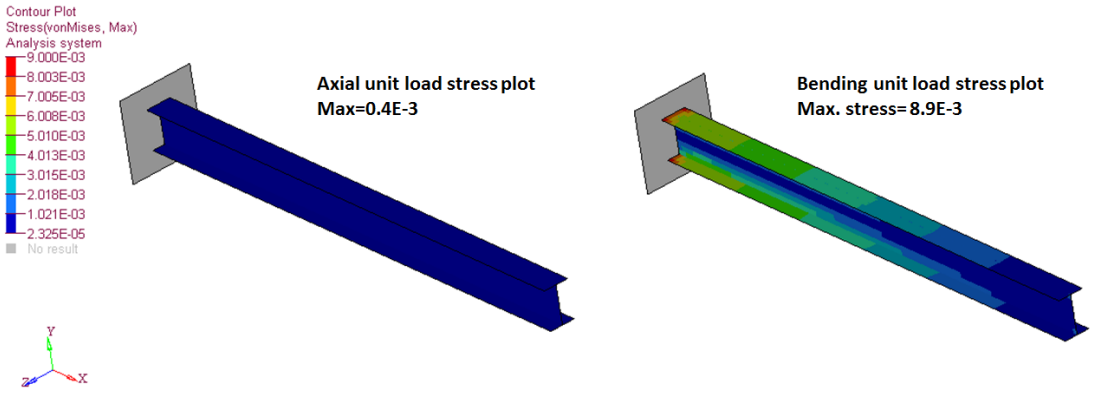

Figure 4.2: Stress plots with axial and bending unit loads

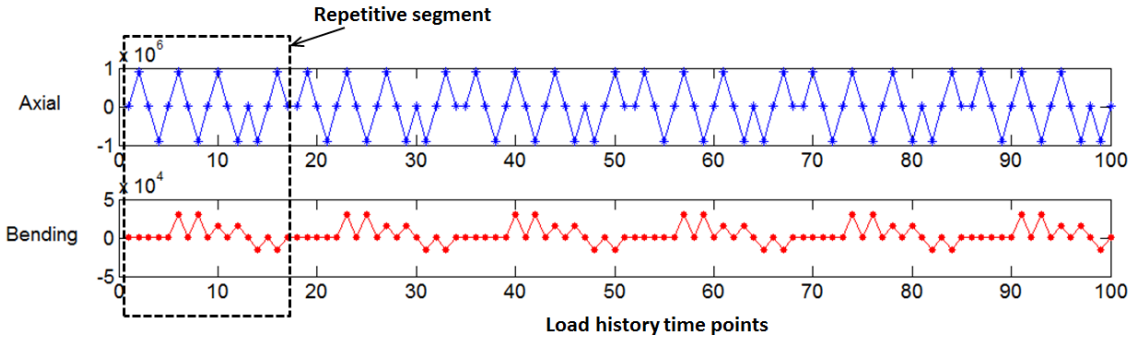

Figure 4.3: Axial and bending load history data

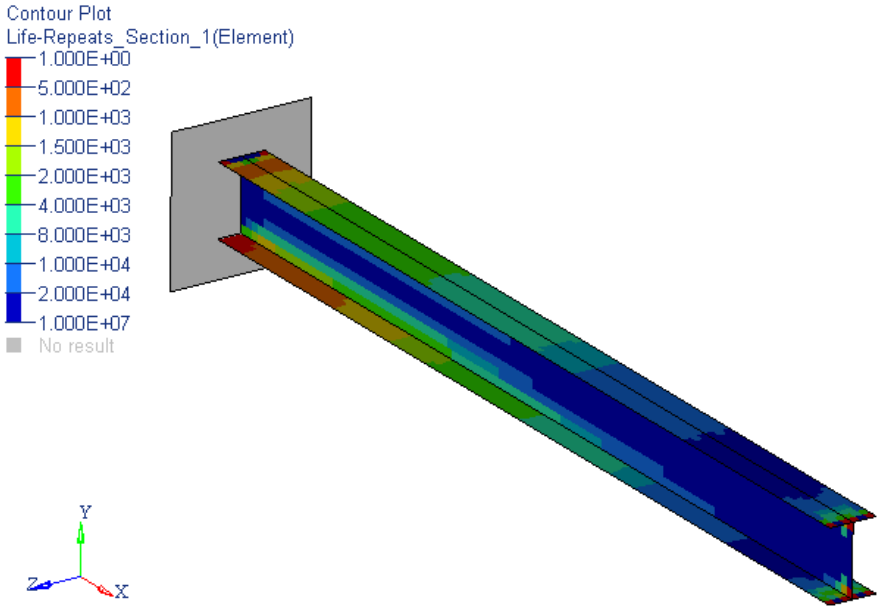

Figure 4.4: Cantilever beam fatigue analysis result

Table 4.1: Fundamental fatigue loads

	Axial (N)	Bending (N)
FFL_01	1800000	45000
FFL_02	1800000	-45000
FFL_03	1800000	0
FFL_04	1800000	30000
FFL_05	1800000	-15000

Since the load history is simple repetitions of the load block, exact fundamental fatigue load (FFL) cases are identified and shown in Table 4.1. In this example, there are five FFLs which account for the fatigue damage. Due to the high magnitudes of axial forces versus bending, the overall NVC values of the loads are close to unit values as shown in Figure 4.5. The NVC results indicate all the load vectors are strongly correlated and can be combined into a single load vector. However, by applying the damage based sensitivity at the fixed boundary condition, the NVC values become more distinctive for finding the patterns of the loads as shown in Figure 4.6. This shows the benefit of using the pattern-amplified fatigue load vectors introduced in the previous section. Based on the damage sensitivity of an observation location, the significance of an individual FFL to the fatigue damage would change. For example, at the location close to the fixed boundary, it is expected the majority of the fatigue damage is from the bending dominant loads, such as FFL_01 and FFL_02 while the axial force, such as FFL_03, will contribute more damage at the locations close to the free end.

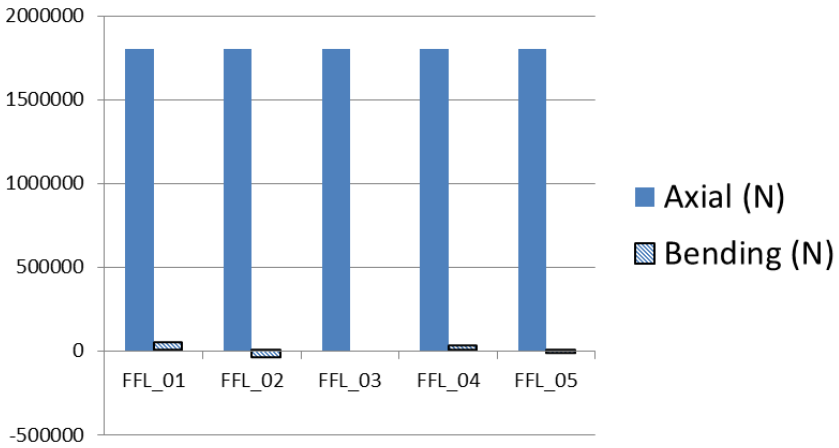

	FFL_01	FFL_02	FFL_03	FFL_04	FFL_05
FFL_01	1	0.9975	0.9994	0.9999	0.9989
FFL_02		1	0.9994	0.9983	0.9997
FFL_03			1	0.9997	0.9999
FFL_04				1	0.9994
FFL_05					1

Figure 4.5: Five FFLs (top) and their NVC values (bottom)

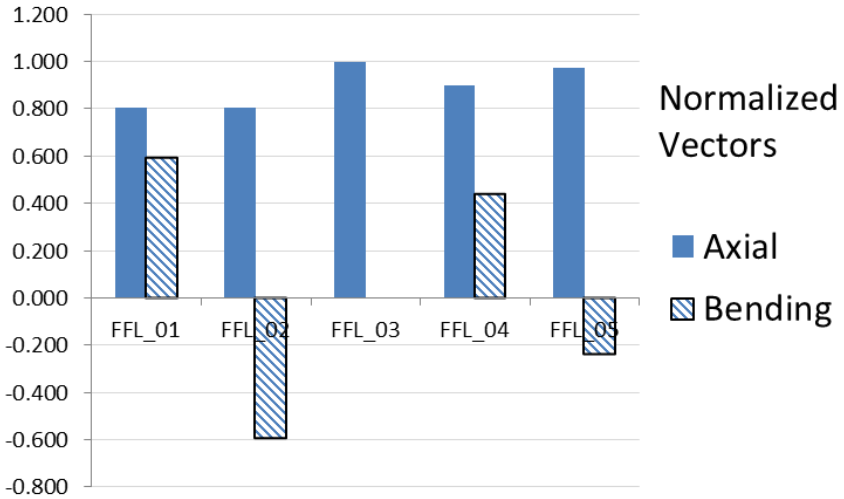

	FFL_01	FFL_02	FFL_03	FFL_04	FFL_05
FFL_01	1	0.087	0.6475	0.9684	0.4089
FFL_02		1	0.6475	0.2117	0.8524
FFL_03			1	0.8053	0.9429
FFL_04				1	0.5867
FFL_05					1

Figure 4.6: Pattern-amplified FFLs (top) and their NVC values (botom)

1) Fundamental fatigue load pattern identification

To find the fundamental fatigue load patterns, a total of 48 observation locations are considered as shown in Figure 4.7. Both the top and bottom sides of marked locations in the figure are considered. In the proposed EDA method, the number of candidate observation locations considered is limited only by the available computational power. The final FFL patterns are obtained by a sequential process of local and global extractions for unique load vector patterns according to the process in Figure 3.3. In this example, the desired damage coverage is set to 98%, which means the worst cycles will be extracted to cover 98% of fatigue damage at each location. The correlation threshold for the local and global pattern identification is 98%. This means if any NVC value of two load vectors is less than 0.98, the vectors are kept as unique load patterns. Having a higher correlation threshold will result more FFL patterns since more LFLVs will be selected as unique load patterns.

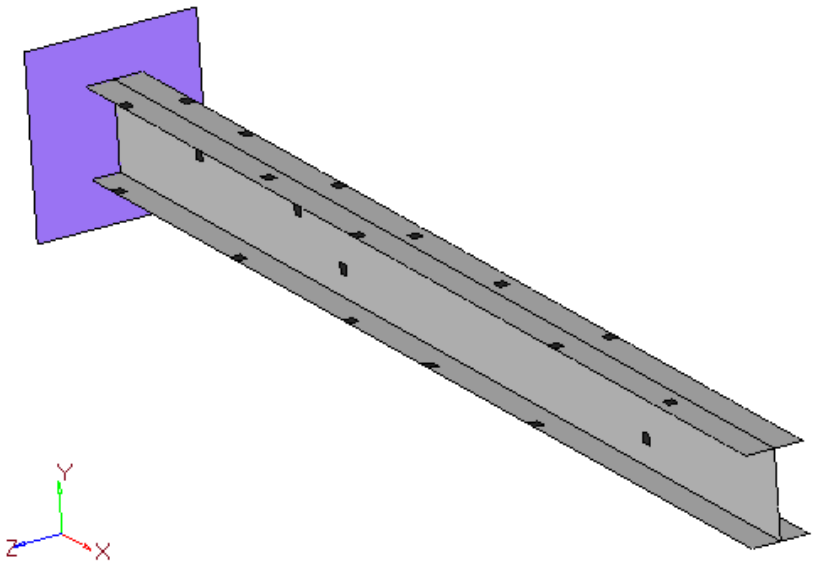

Figure 4.7: Candidate observation locations (marked with black squares)

Case study 1: With low fatigue life coverage, it can be expected less significant worst cycles would be ignored in the EDA process. Figure 4.8 shows the case study result with 90% fatigue life coverage. The FFL_05, which is less damaging than other FFLs, is not selected as a unique load pattern. Therefore, by varying the fatigue life coverage and performing the EDA process, sensitivities of fundamental fatigue load patterns to the fatigue damage can be estimated.

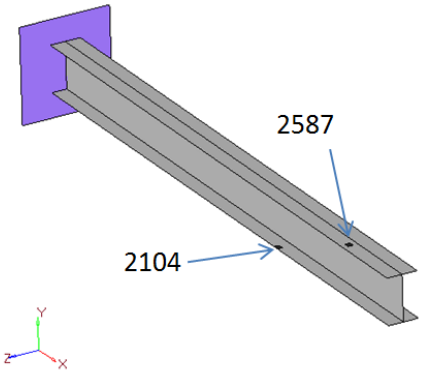

Fatigue life coverage = 90%
Pattern search threshold = 98%

Sensor Location EID: 2104

FFL coverage

FFL_01	1800000	45000
FFL_03	1800000	0

Sensor Location EID: 2587

FFL coverage

FFL_02	1800000	-45000
FFL_04	1800000	30000

Figure 4.8: Case study 1 - FFL patterns result w/ fatigue life coverage 90%

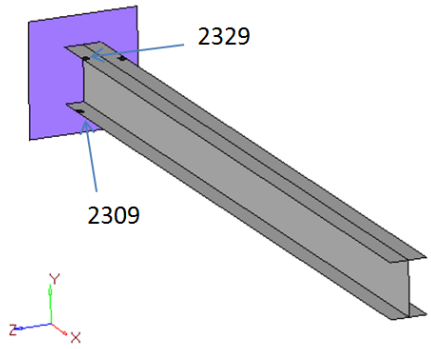

Fatigue life coverage = 98%
Pattern search threshold = 98%

Sensor Location EID: 2309

FFL coverage

FFL_01	1800000	45000

Sensor Location EID: 2329

FFL coverage

FFL_02	1800000	-45000

Figure 4.9: Case study 2 - FFL patterns result w/ fatigue life coverage 98%

Case study 2: When the set of observation locations are limited only on the area close to the fixed boundary, even though the fatigue life coverage is back up to 98% as before, it is expected to find only FFLs with high bending loads. Figure 4.9 shows the expected result which lists only FFL_01 and FFL_02 as fundamental load patterns. It shows if observation locations are set to only the locations of high fatigue damage, it could potentially miss some other fundamental fatigue load contents. Therefore, to extract fatigue design loads, the observation locations should be considered from the perspective of capturing fatigue load patterns rather than high fatigue damages.

2) Fatigue design load transformation

Once the fundamental fatigue load patterns are obtained, the goal turns out to be the identification of the small set of fatigue design loads instead of the complicated full set of loading history, which produces the exact match of fatigue damage throughout the structure. In order to demonstrate the efficiency of this methodology, 4 locations are chosen randomly throughout the cantilever beam, shown in Figure 4.10. Simplified full loading history is defined as 1000 repeats of the repetitive segment shown in Figure 4.3. After the fundamental fatigue load pattern identification, three load patterns are detected, which captures 98% of the fatigue damage in each observation location. Figure 4.11. shows the three load patterns within one repetitive segment by connecting the load history time points. In this example, since bending causes much more damage on the structure than the axial loading, it could be considered that FFL 1 and FFL 2 mainly capture the bending, but in different directions, while FFL 3 reflects only axial loading.

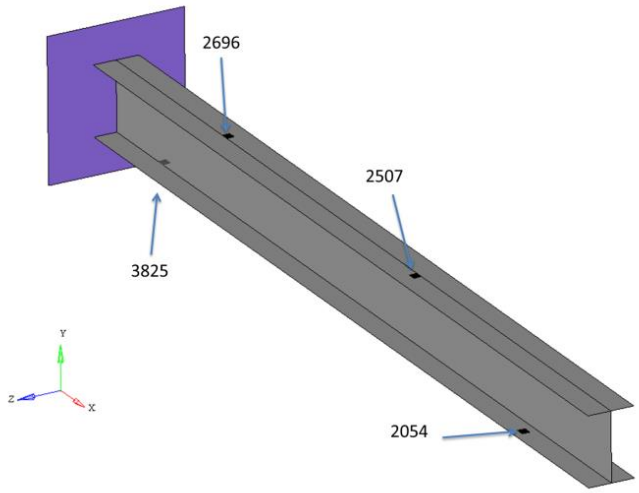

Figure 4.10: Candidate observation locations for fatigue design load development

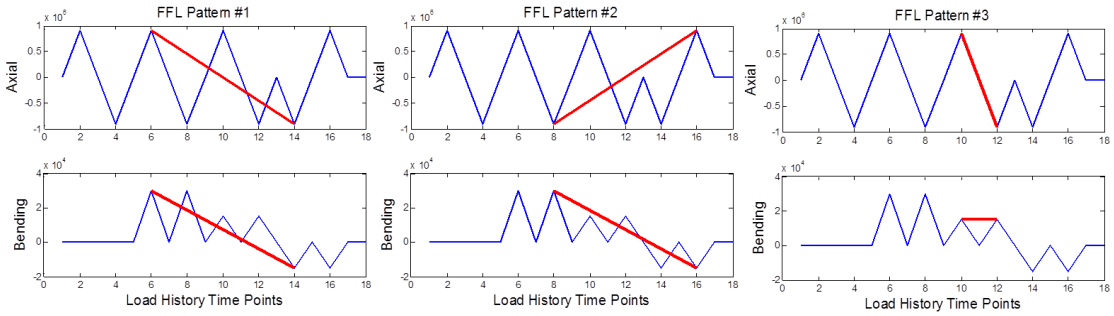

Figure 4.11: Fundamental fatigue load patterns within one repetitive segment loading

By performing EDA again, all correlated local fatigue load vectors are extracted from the association information (Eq. 3.18) from fatigue load pattern identification. Since the loading history is repetitive with the single segment, the same fundamental fatigue load patterns detected within segments are repeated throughout the load history. Initial scales and frequencies are easily determined with FFL patterns of uniform distribution.

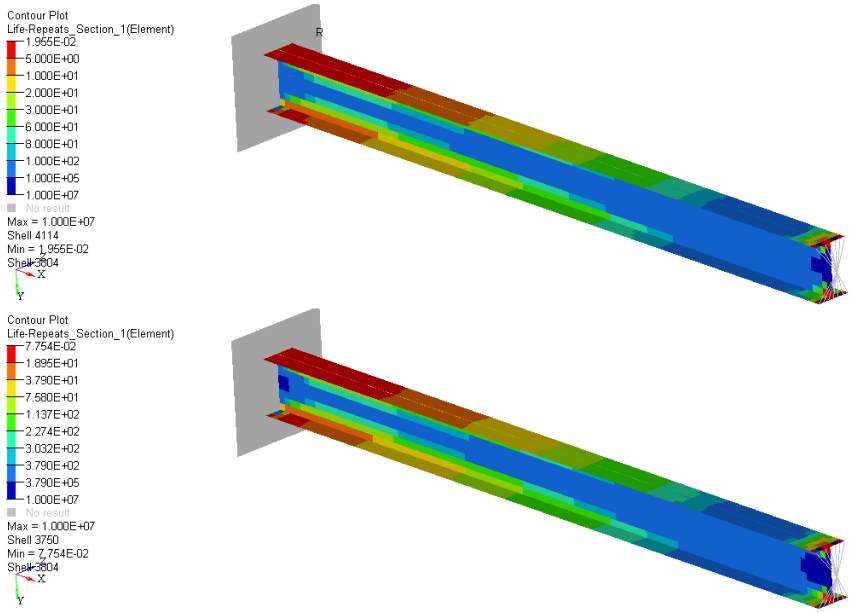

Figure 4.12: Fatigue contour comparison between full loading (top)

and optimum scales (bottom)

Scale optimization is performed by combining normalized fatigue damage for four locations to get the relative match of fatigue damage, choosing element 2054 as the reference location. Optimization is performed using MATLAB optimizer. Figure 4.12 is the relative fatigue life contour comparison between full loading and optimum scale with initial frequency by adjusting the legend of the contour plot. After the first stage of optimization, the relative matching of fatigue contour is achieved by capturing most of the features on the four observation locations. Table 4.2 shows the comparison of the fatigue analysis results of observation locations and the relative ratios with respect to the

response on element 2054. The relative error of the ratio for each location is improved quite massively after optimization.

Table 4.2: Relative fatigue life comparison

	Full Loading		Initial Scales (1.0,1.0,1.0)			Optimum Scales (0.846, 0.845, 0.913)		
Element	**Target life**	**Ratio**	**Initial life**	**Ratio**	**Error**	**Optimum life**	**Ratio**	**Error**
2054	134.16	100.000%	145.21	100.00%	0.00%	508.98	100.000%	0.00%
2507	66.577	49.625%	66.732	45.96%	7.39%	247.53	48.633%	2.00%
2696	12.816	9.553%	12.299	8.47%	11.34%	48.657	9.560%	0.07%
3825	2.8628	2.134%	2.7349	1.88%	11.74%	10.861	2.134%	0.00%

After getting the relative match of fatigue damage all over the structure, frequency optimization is performed to get the exact match of the fatigue damage for the four observation locations. The optimum scales are fixed. Once the optimization is finished, optimum frequencies along with the optimum scales are regarded as the fatigue design loads. Figure 4.13 shows the comparison of fatigue contour between full loading history and fatigue design loads using the same legend. Table 4.3 shows the fatigue life of all observation locations for both full loading and fatigue design loads. Table 4.4 shows the fatigue design loads.

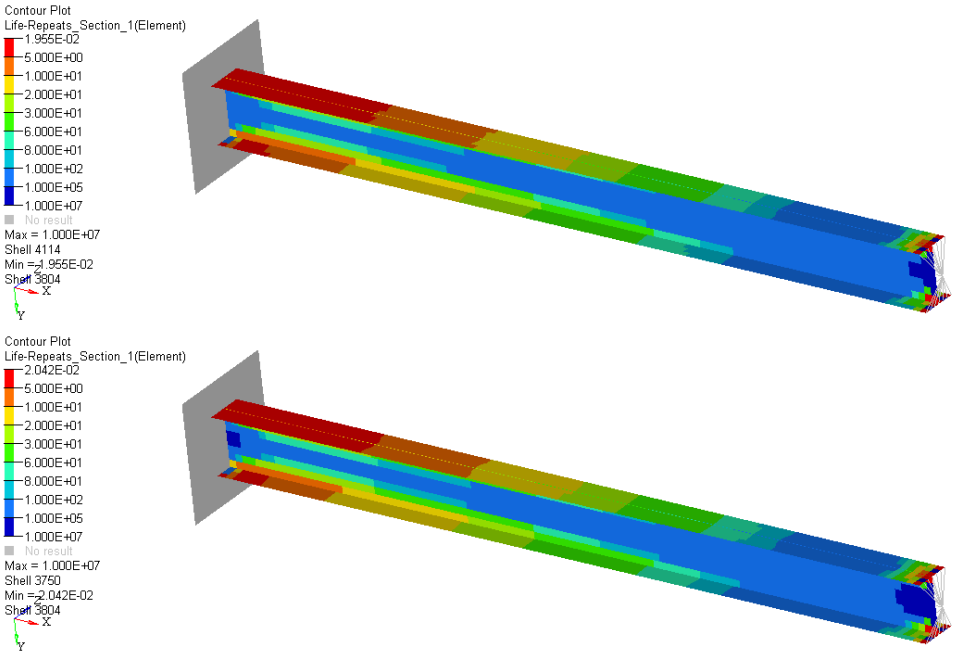

Figure 4.13: Fatigue contour comparison between full loading (top) and fatigue design loads (bottom)

Table 4.3: Fatigue Life Comparison between full loading and fatigue design loads

	Full Loading	Fatigue Design Loads	
Element	**Target life**	**Optimum life**	**Error**
2054	134.16	134.7	0.40%
2507	66.577	65.919	0.99%
2696	12.816	12.952	1.06%
3825	2.8628	2.8606	0.08%

Table 4.4: Fatigue design loads

FFL pattern	Scale	Frequency
1	0.846	3797
2	0.845	3757
3	0.913	3742

Figure 4.14: General hydraulic excavator and its front linkage boom structure

4.1.2 Industrial example: hydraulic excavator front linkage structure

To demonstrate the practicality of the proposed EDA framework for an industrial scale problem, the front linkage structure of a hydraulic excavator as shown in Figure 4.14 is presented in this section. A general Excavator has three parts of front linkage bodies, usually referred to as a boom, stick, and bucket, which are actuated by three main hydraulic cylinders. The boom structure, which is the first linkage body from the rotating platform, will be investigated for the fatigue design load determination. The linkage point tagged as PT1 in the boom figure is the hinge joint on the main platform, PT2 is for a boom cylinder, PT3 for a stick cylinder, and PT4 is the linkage connection to the stick

structure. The boom cylinder makes vertical motions, while the stick cylinder is usually for digging in and out. With many different configurations of the front linkage, excavators can perform many different tasks. One of the common applications is truck loading in which an excavator loads material on a truck as shown in Figure 4.14. The truck loading consists of several operations, such as digging, lifting, rotating, dumping, and returning. During the course of this operation, the boom structure will be under different loadings coming from the main platform vibrations with a counter weight mass, as well as from soil to bucket interactions. For the boom structure, there are a total of 14 load channels as shown below in Table 4.5 where, for example, PT1FX and PT1MX stand for force and moment components in the x direction, respectively. Figure 4.15 shows typical load histories at a few selected channels for the truck loading application data. In a typical design process, structural yielding loads defined from extreme operations are used for concept design exploration. However, fatigue damage failures, which are different from yield failures, would not be addressed correctly unless the yield loads are the same as the fatigue loads embedded in the load history data. Therefore, by using the proposed EDA method, the fundamental damage loads from the load history are extracted and applied in the concept design development of the boom structure. In this example, there are basically two processes. The Process I is used to demonstrate the fundamental fatigue design load patterns from different damage coverage and correlation threshold with randomly selected gages though out the structure, which is documented in a paper by Bae at al. [10]. Fatigue design load transformation is the Process II shown in the following part with virtual gage locations focusing on the high damaged area all over the structure.

Table 4.5: Load channel names for the boom structure

PT1	PT2	PT3	PT4
PT1FX	PT2FX	PT3FX	PT1FX
PT1FY	PT2FY	PT3FY	PT1FY
PT1FZ			PT1FZ
PT1MX			PT1MX
PT1MY			PT1MY

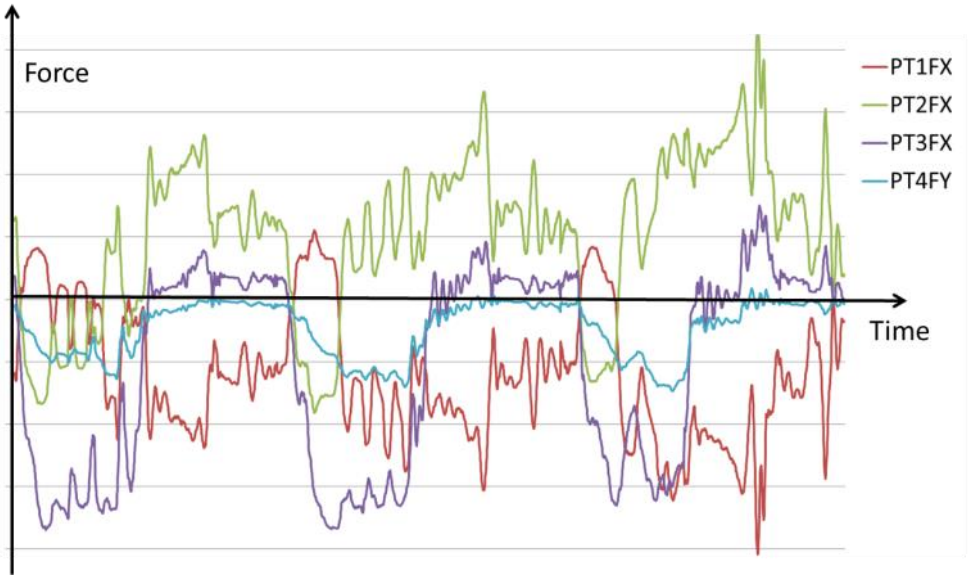

Figure 4.15: Load history for truck loading application

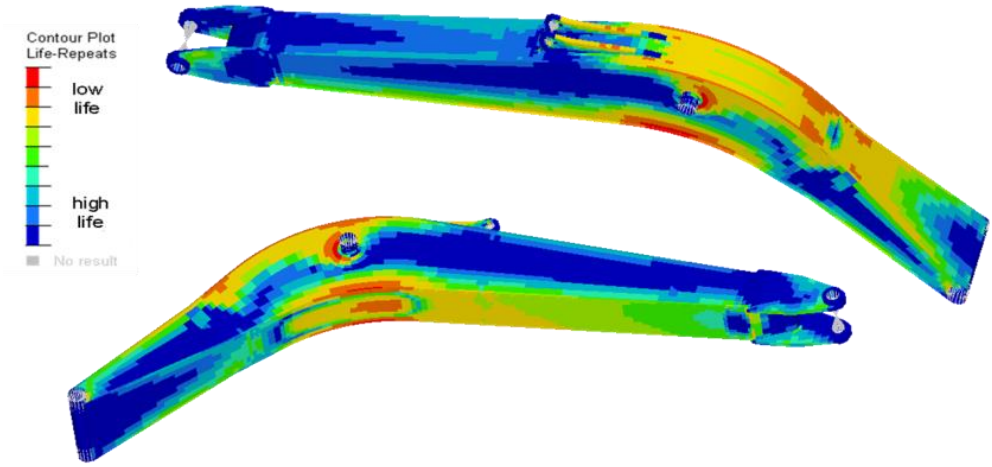

Figure 4.16: Fatigue life contour with the given load history

As in the previous example, the structural fatigue life contour is assessed by using the multi-axial principal stress algorithm with ISO steel 1020 as shown in Figure 4.16. For the sake of detecting major fatigue design loads to capture most of the severe damage, 44 virtual gages are chosen all over the boom structure focusing on area with low fatigue life applying full loading conditions, which are shown in Figure 4.17. If computational power is allowed, we can choose locations of as many as we can. After going through Process I to identify fundamental fatigue load patterns with 95% of damage coverage and 98% of pattern search threshold, 30 FFL patterns are detected as unique ones, which means these 30 load patterns will account for 95% of the total damage of each virtual gage location with a correlation smaller than 98%.

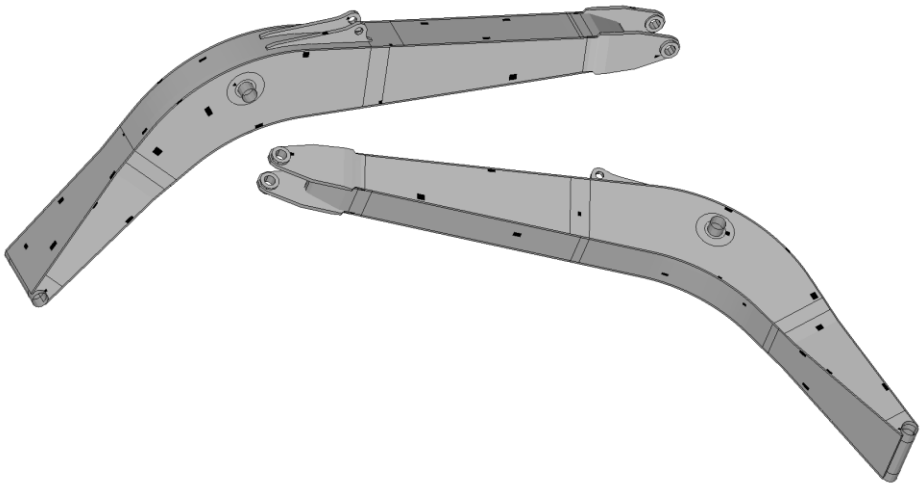

Figure 4.17: 44 Virtual gage locations (marked with black squares)

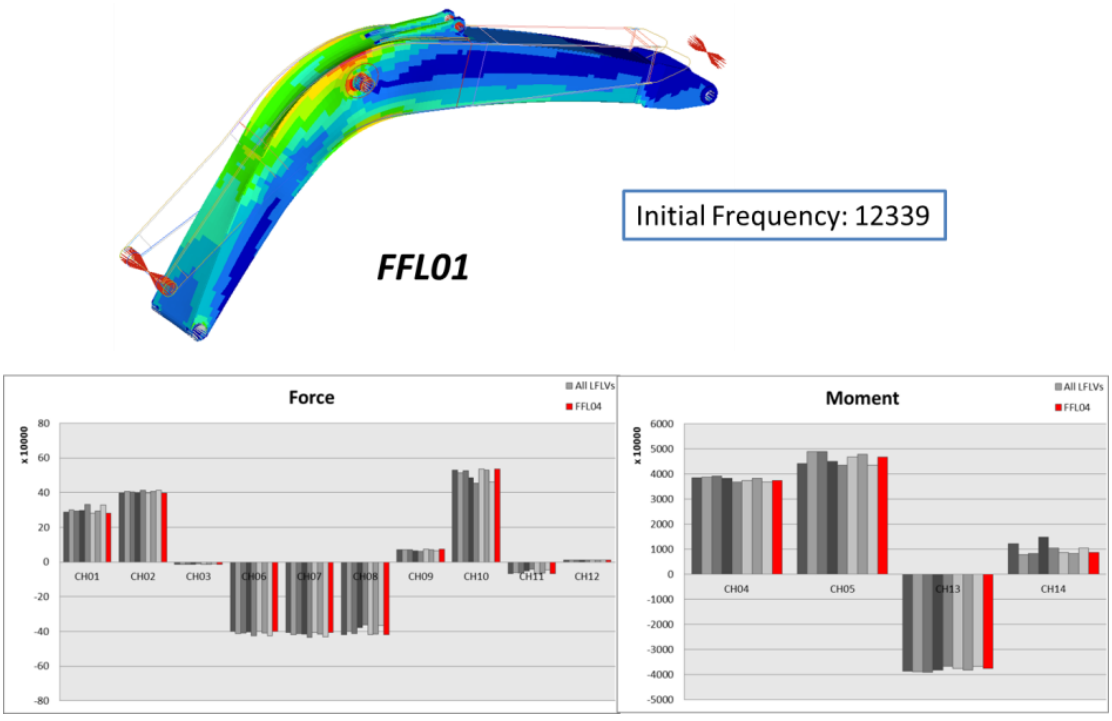

Figure 4.18: Initial value determination (FFL01)

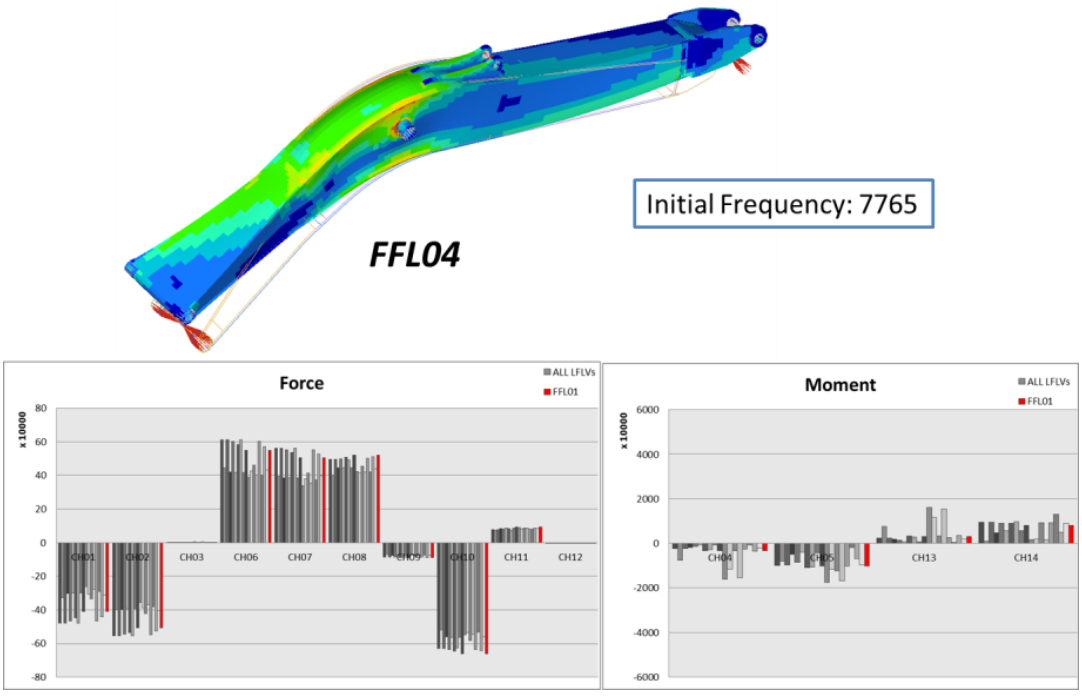

Figure 4.19: Initial value determination (FFL04)

For the two-stage optimizations of transforming fatigue design loads, initial scales and frequencies are determined by EDA and optimization techniques. All correlated local fatigue load vectors are extracted from association information (Eq. 3.18) kept in the stage of pattern search. Initial scales are determined by EDA to find the median values through statistical study. On the other hand, initial frequencies, which basically cause the fatigue damage approximately as the one applying all correlated local fatigue load vectors throughout all virtual gages along with the initial scales, are achieved by solving optimization problems defined by Eq. 3.19. Figure 4.18 and 4.19 show the deformed shape and all correlated local fatigue load vectors (LFLVs) of FFL01 and FFL04, respectively. The red bar represents the initial scale of each channel. Initial frequencies for FFL01 and FFL04 are 12339 and 7765. Figure 4.20 is the fatigue life contour

comparison between full loading history and the initial conditions. As it shows, the relative match is obtained for most of the region of the structure except for some areas, such as the area within the red circle, which will be addressed in the two-stage optimizations.

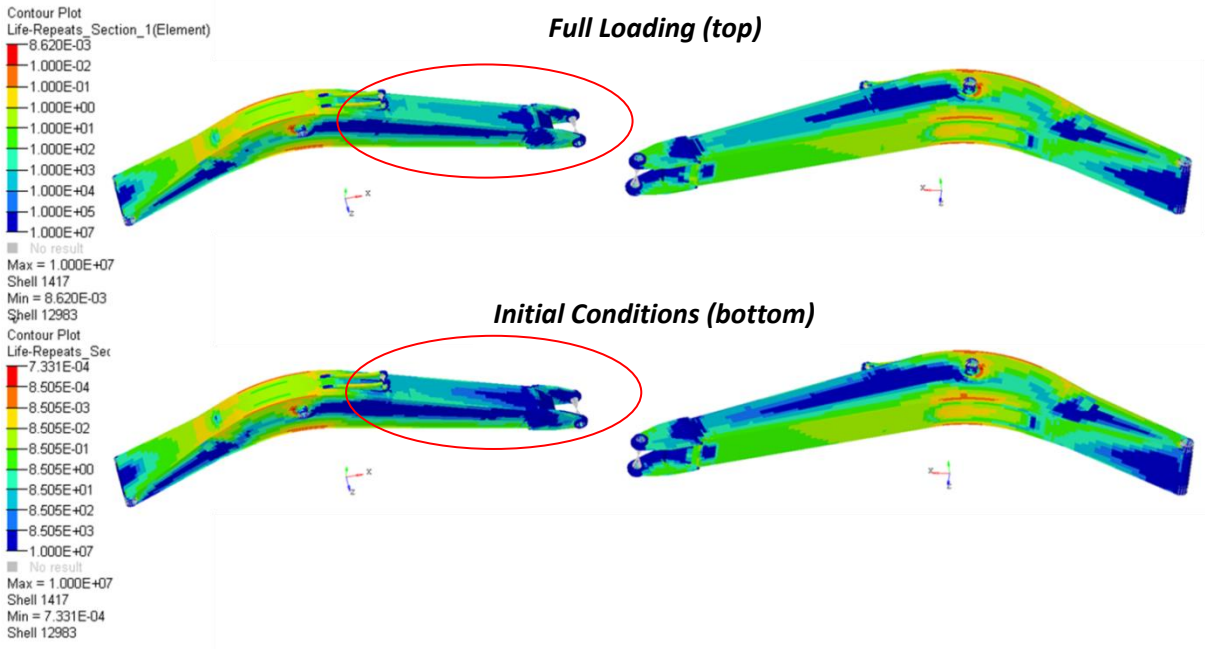

Figure 4.20: Fatigue contour comparison between full loading history (top) and initial conditions (bottom)

In order to obtain relative damage match throughout all 44 virtual gages, scale optimization is performed using a gradient based method according to the formulation in Eq. 3.20, in which there are 30 design variables. Converged solutions are found after 29 iterations shown in Figure 4.21 with iteration history of objective function and some design variables. The region within the red circle with bad contour match in initial conditions is improved shown in Figure 4.22. This is still relative match since the legends of full loading history and optimum results are not the same.

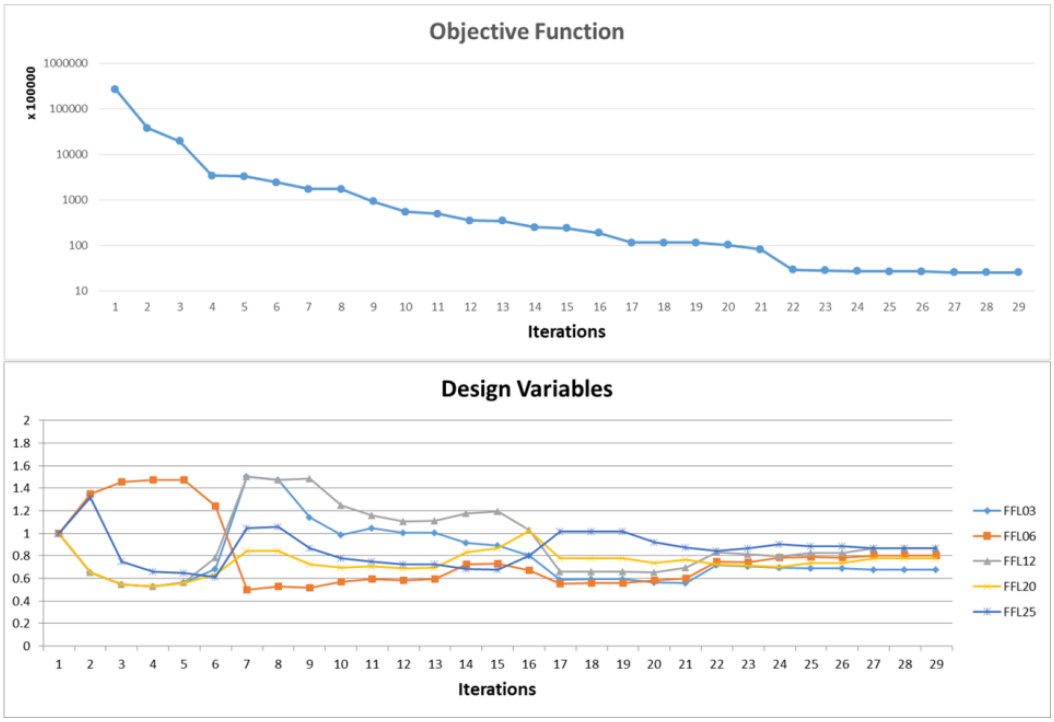

Figure 4.21: Iteration history of scale optimization

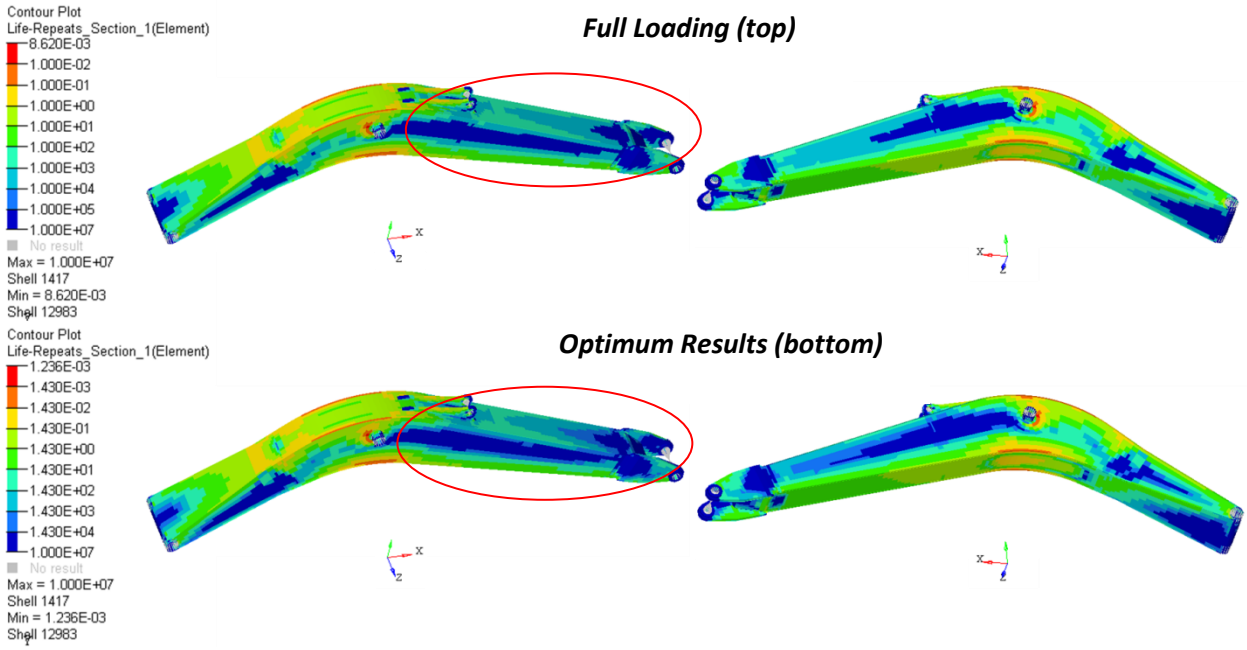

Figure 4.22: Fatigue contour comparison between full loading history (top) and scale optimum results (bottom)

Our goal is to get absolute fatigue damage match all over the structure which is addressed by adjusting frequencies up and down in the second stage of optimization (Eq. 3.21), thus, frequencies are the design variables. Fatigue life contour comparison between full loading history and the optimization results is shown in Figure 4.23. The legends are the same and good correlation results are achieved, which means, by applying these 30 fatigue design loads only, fatigue damage can be regenerated throughout the structure instead of applying the full loading history that has more than 10,000 data points. It does reduce the computational time to run fatigue analysis simulation. More designs can be explored within given time. However, the most valuable benefits are the understandings and insights on fatigue damage from finite sets of fatigue design load.

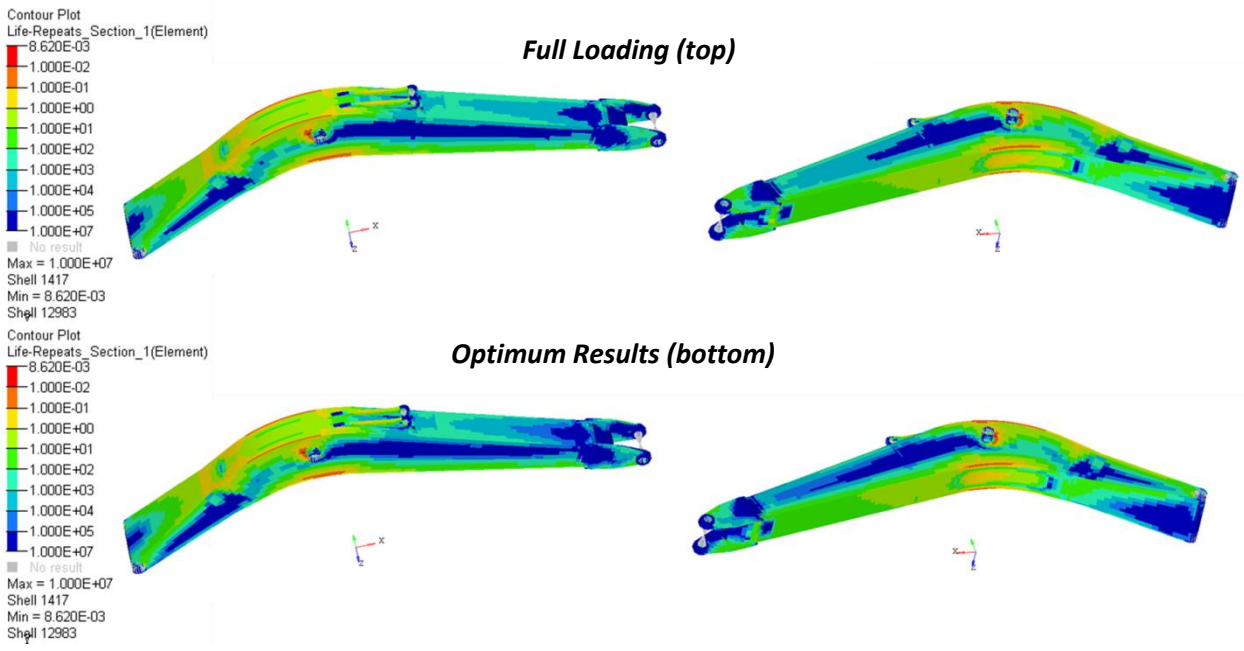

Figure 4.23: Fatigue contour comparison between full loading history (top) and frequency optimum results (bottom)

In reality, fabrication weldings of the structure are more susceptible to fatigue failure than other locations. After fatigue design loads are determined, better understandings and insights of structural damage mechanism can be extracted by looking at each virtual gage locations. Element 10386, for example, is located at the edge of the boom structure which is the hot spot where typical welding fatigue failure happens very often, shown in Figure 4.24. By applying the fatigue design loads, it is clear that these three types of loadings account more than 93% of damage at that location. Therefore, if the structural design around that area needs to be improved, the main considerations should be focused on these three types of critical loads. Also, the quantitative damage contribution of each type of load can be extracted shown in Table 4.6. These will be useful information for design engineers which they can never get from full loading data.

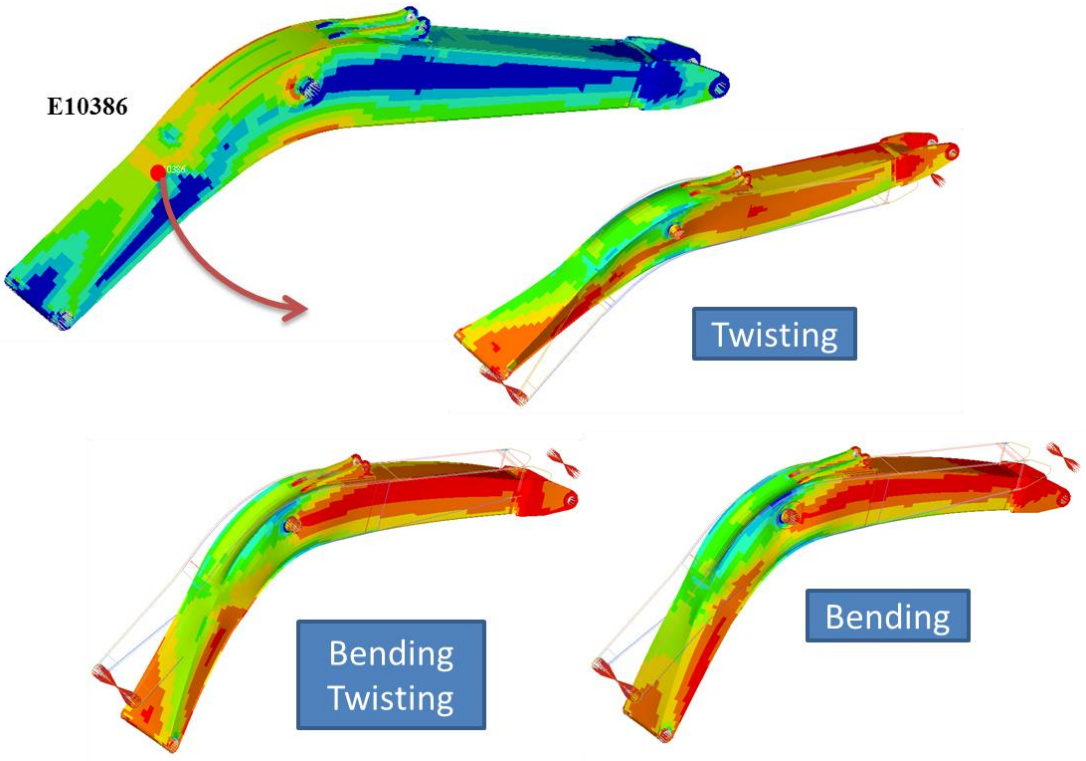

Figure 4.24: Damage mechanism extraction on welding areas

Table 4.6: Quantitative damage contributions

FFL #	Load Type	Severity	Damage
FFL01, FFL07, FFL10, FFL22	Bending	64.51%	93.41%
FFL08	Bending+Twisting	22.29%	
FFL21	Twisting	6.62%	

4.2 Cantilever beam robust design by Taguchi optimization toolkit

Taguchi design is applied on a cantilever beam test problem shown in Figure 4.25. w, t and L are the width, height and length of the cantilever beam. X and Y are the horizontal and vertical forces applied on the tip of the beam. E is the Young's modulus. V_0 and D_0 are the targeted volume and upper bounds of tip displacement. The analytical equations for volume and displacement are shown below in Eq. 4.1 and 4.2, respectively.

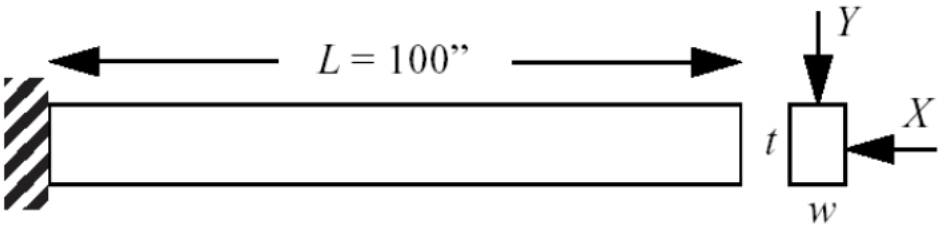

Figure 4.25: Cantilever beam test problem

$$volume = w \times t \times L = V_0 \tag{4.1}$$

$$displacement = \frac{4L^3}{Ewt}\sqrt{\left(\frac{Y}{t^2}\right)^2 + \left(\frac{X}{w^2}\right)^2} \le D_0 \tag{4.2}$$

Table 4.7: Parameters for Taguchi design

	Variable	Type	Constraint	Variation
w	Width	**Design Parameter**	1.0 < w <10.0 inches	**2.45%**
t	Thickness	**Design Parameter**	1.0 < t <10.0 inches	**2.45%**
X	Horizontal Force	Random	X = 500 lbf	**9.80%**
E	Young's Modulus	Random	E = 2.9e7 psi	**12.25%**
L	Length	Fixed	100 inches	Negligible

Table 4.8: Orthogonal Array for control factors

Experimental Runs	Control Factor (Levels)	
	w (3)	t (3)
1	1	1
2	1	2
3	1	3
4	2	1
5	2	2
6	2	3
7	3	1
8	3	2
9	3	3

Table 4.7 shows all the related parameters for this example. It is clear that there are two design parameters, or control factors and four noise factors. Because of the machinery error, width and thickness are both control factors and noise factors. The other two noise factors are horizontal force and Young's Modulus coming from the uncertainty in loading conditions and material properties. The targeted volume of the cantilever beam

should be V_0 $(800\ in^2)$ and the displacement should be smaller than D_0 $(2.20\ in)$. There are three levels for each control and noise parameters. L9 Orthogonal Arrays are used for both control and noise factors shown in Table 4.8 and 4.9.

Table 4.9: Orthogonal Array for noise factors

Experimental Runs	Noise Factor (Levels)			
	w (3)	t (3)	X (3)	E (3)
1	1	1	1	1
2	1	2	2	2
3	1	3	3	3
4	2	1	2	3
5	2	2	3	1
6	2	3	1	2
7	3	1	3	2
8	3	2	1	3
9	3	3	2	1

Assume the initial designs are 3 inches for both width and thickness. The first local range is 50% of the total design domain based on the initial starting points. Designs of experiments are performed according to the Orthogonal Array. Nominal-the-best is chosen as the SN ratio. Least square model with interaction term is used as the regression model for both responses and SN ratio. The objective is to maximize combined SN ratio of both volume and displacement with weights 80% and 20%, respectively. Every time the criterial for updating local window meets, the local window for next iteration will become 70% of the current one. The following figure shows the user's inputs used for the Python toolkit for Taguchi design.

```
##Variables
control factors
#Initial Value, Lower Bounds, Upper Bounds, Levels, Name
3.0     1.0     10.0    3       w
3.0     1.0     10.0    3       t


noise factors
#Lower Bounds, Upper Bounds, Levels, Name
0.9755051       1.0244949       3       w
0.9755051       1.0244949       3       t
0.9020204       1.0979796       3       X
0.8775255       1.1224745       3       E


##responses
responses
#Lower Bounds, Upper Bounds, Weight for SN, Name
800.0   800.0   0.8     Volume
NaN     2.20    0.2     Displacement


##Run Process
least square interaction term
#'on' or 'off'
on


SN option
#1: smaller-the-better  2: larger-the-better    3: nominal-the-best
3       3


Confirmation run option
#1: response fun        2: least square approximation
1


CF matrix
1       1
1       2
1       3
2       1
2       2
2       3
3       1
3       2
3       3
```

```
NF matrix
1       1       1       1
1       2       2       2
1       3       3       3
2       1       2       3
2       2       3       1
2       3       1       2
3       1       3       2
3       2       1       3
3       3       2       1


max iteration
50


local range ratio
0.5


local range update ratio
0.7


edge percentage for updating local range
0.02


termination ratio
#CFs    Funs
0.001   0.005


number differences check
3


opt_max_iteration
100


opt_convergence_tolerance
1.0e-8
```

Figure 4.26: User's inputs for Taguchi design toolkit

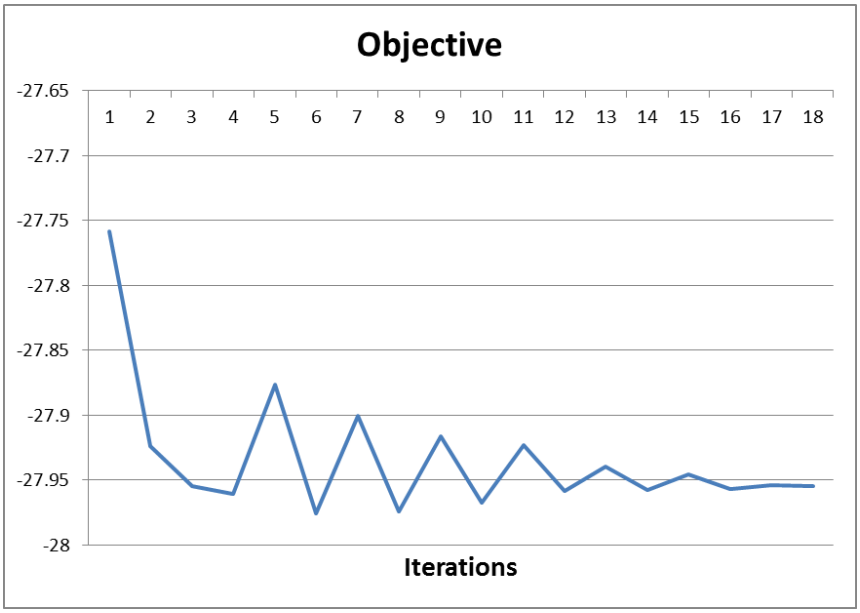

Figure 4.27: Iteration history – objective function

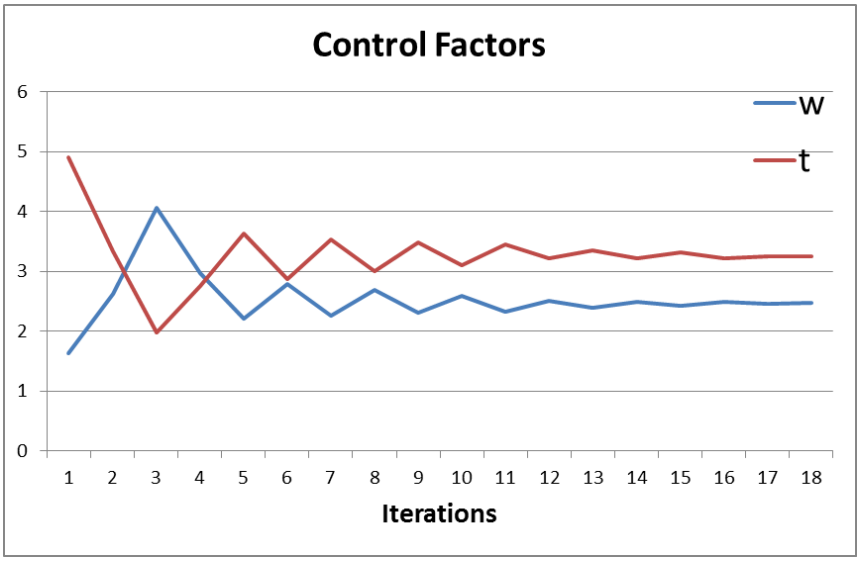

Figure 4.28: Iteration history – control factors

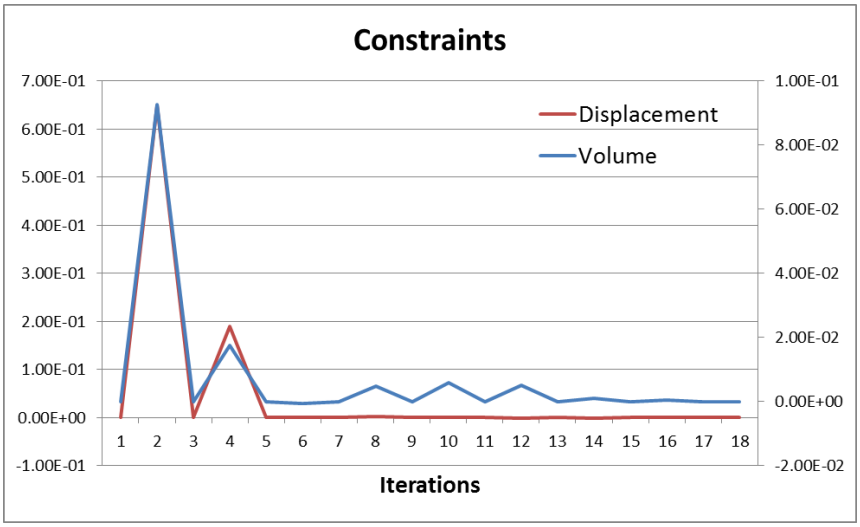

Figure 4.29: Iteration history – constraints

Figure 4.27 – 4.29 show the iteration history for objective function, control factors, and constraints. After 18 iterations, converged solutions are obtained. The optimization results are shown in Table 4.10. It turns out that the optimum volume hits the target and the displacement is within the bounds.

Table 4.10: Taguchi optimization results

Variable	Value
w	2.467
t	3.242
S/N ratio	27.955
Confirmed Volume	800
Confirmed Displacement	2.197

5. Summary and future work

5.1 Research summary

Engineering Data Analytics (EDA) approach to extract fatigue design load by leveraging large amount of measured load data was proposed by this research work. There are basically two processes for this method: 1) Fundamental fatigue load pattern identification, 2) Fatigue design load transformation. Data analytics and physics based engineering mechanics are combined to detect fundamental fatigue load patterns through a two-level search algorithm. Damage based sensitivity weights are applied for the Normal Vector Correlation (NVC)-based pattern mining to amplify unique load patterns. Fundamental fatigue load patterns are transformed into a practical fatigue design load set via inverse optimization. The optimization will be performed with a two-stage process with an initial design configuration determined through the proposed EDA. The proposed methodology was successfully demonstrated with the industrial scale structural design problem, the front linkage structure of hydraulic excavator. Useful and important information for design engineers to make decision for structural design can be extracted from this process. It turns out that the proposed framework is a transferable, repeatable and applicable process for young engineers without much expertise and experience. It can also be utilized to solve general engineering design challenges in various industries, such as automotive, aerospace, health-care, energy, and etc.

The proposed Taguchi optimization toolkit with moving window strategy turns out to be an effective way to reduce experimental time and computational cost. Design of experiments is performed based on the chosen Orthogonal Array within a moving and

changing local window. Multi-responses robust design is achieved by maximizing the S/N ratio after the data analytics. The moving window strategy locates the targeted design domain at the beginning with a large window. Then, the local window keeps becoming smaller till focus on the accurate and converged optimization results.

5.2 Future work

As a next step of the study, to increase the effectiveness of the EDA process to a large-size and complex problem, the proposed design load development method will be applied to numerical examples to demonstrate the availability. The practical considerations, such as the number of observation locations to choose, the computational time to perform this process, and choice of numerical optimization strategy, will be investigated next. This methodology can be extended to develop fundamental fatigue design loads that can replace the full measured load in estimating structural durability in an effective and efficient manner, especially targeting application in the concept design development. Also, as more measured data sets are collected for the similar group of machine operations, statistical inference of fatigue design loads can be obtained to address robustness based concept design against uncontrollable variability in real operational conditions.

6. Bibliography

[1] Dieter, G. E. and Schmidt, L. C., *Engineering Design*, 5th ed., McGraw-Hill, New York, NY, 2013

[2] Wang, L., Shen, W., Xie, H., Neelamkavil, J., and Pardasani, A., "Collaborative conceptual design – state of the art and future trends", *Computer-Aided Design*, Vol. 34, 2002, pp. 981-996

[3] Kang, B. S., Park, G. J. and Arora, J. S., "Optimization of flexible multibody dynamic systems using equivalent static load method," *AIAA Journal*, Vol. 43, No. 4, April 2005, pp. 846 – 852.

[4] Park, K. J., Lee, J. N., and Park, G. J., "Structural shape optimization using equivalent static loads transformed from dynamic loads," *International Journal of Numerical Methods in Engineering*, Vol. 63, 2005, pp. 589 – 602.

[5] Wickham, M. J., Riley, D. R. and Nachtsheim, C. J., "Integrating Optimal Experimental Design into the Design of a Multi-Axis Load Transducer," *Journal of engineering for industry*, Vol. 117, 1995, pp. 400-405.

[6] Oh, C. S., "Application of wavelet transform in fatigue history editing," *International Journal of Fatigue*, Vol. 23, 2001, pp. 241 – 250.

[7] Abdullah, S., Choi, J. C., Giacomin, J. A., and Yates, J. R., "Bump extraction algorithm for variable amplitude fatigue loading," *International Journal of Fatigue*, Vol. 28, 2006, pp. 675 – 691.

[8] Packianather, M. S., Drake, P. R., and Rowlands. H., "Optimizing the parameters of multilayered feedforward neural networks through Taguchi design of

experiments." *Quality and reliability engineering international*, Vol. 16, No. 6, 2000, pp. 461-473.

[9] Zhang, J. Z., Chen, J. C., and Kirby, E. D., "Surface roughness optimization in an end-milling operation using the Taguchi design method." *Journal of materials processing technology*, Vol. 184, No. 1, 2007, pp. 233-239.

[10] Bae, H., Ando, H., Nam, S., Kim, S. and Ha, C., "Sensor (monitoring points) layout method for fatigue design load extraction," *Proceedings of 54th AIAA/ASME/ASCE/AHS/ASC Structures, Structural Dynamics, and Materials Conference*, AIAA 2013-1691, Boston, Massachusetts, 2013.

[11] Beck, J. V., and Woodbury K. A., "Inverse problems and parameter estimation: integration of measurements and analysis." *Measurement Science and Technology*, Vol. 9, No. 6, 1998, pp. 839-847.

[12] Chiwiacowsky, L. D., and de Campos Velho, H. F., "Different approaches for the solution of a backward heat conduction problem." *Inverse Problems in Engineering*, Vol. 11, No. 6, 2003, pp. 471-494.

[13] Uhl, T., "The inverse identification problem and its technical application." *Archive of Applied Mechanics* Vol. 77, No.5, 2007, pp. 325-337.

[14] Tikhonov, A. N., and Arsenin V. Y., *Solutions of ill-posed problems*, Winston and Sons, Washington ,DC, 1977.

[15] Haber, E., Ascher, U. M., and Oldenburg, D., "On optimization techniques for solving nonlinear inverse problems." *Inverse problems*, Vol. 16, No. 5, 2000, pp. 1263-1280.

[16] Holland, J. H., *Adaptation in natural and artificial systems: An introductory analysis with applications to biology, control, and artificial intelligence*. University of Michigan Press, Ann Arbor, 1975.

[17] Hill, M. C., *Methods and guidelines for effective model calibration*. Denver, CO, USA: US Geological Survey, 1998.

[18] Miner, M. A., "Cumulative damage in fatigue," *Journal of Applied Mechanics*, Vol. 12, Trans ASME Vol. 67, 1945, pp. A159-A164.

[19] Downing, S. D., and Socie, D. F. "Simple rainflow counting algorithms," *International Journal of Fatigue*, Vol. 4, No. 1, 1982, pp. 31–40.

[20] Haiba, M., Barton, D. C., Brooks, P. C., and Levesley, M. C. "Review of life assessment techniques applied to dynamically loaded automotive components," *Computers and Structures*, Vol. 80, 2002, pp. 481–494.

[21] Huang, L., Agrawal, H., and Kurudiyara, P., "Dynamic durability analysis of automotive structures," *Society of Automotive Engineering*, SAE paper 980695, 1998.

[22] Conle, F. A. and Mousseau, C. W., "Using vehicle dynamics simulations and finite-element results to generate fatigue life contours for chassis components," *International Journal of Fatigue*, Vol. 13, No. 3, 1991, pp. 195–205.

[23] Socie, D. F., "Multiaxial fatigue damage models," *Journal of Engineering Materials and Technology*, Vol. 109, 1987, pp. 293–298.

[24] Lazzarin, P., and Susmel, L., "A stress-based method to predict lifetime under multiaxial fatigue loadings," *Fatigue and Fracture of Engineering Materials and Structures*, Vol 26, 2003, pp. 1171–1187.

[25] Liu, Y., and Mahadevan, S., "Multiaxial high-cycle fatigue criterion and life prediction for metals," *International Journal of Fatigue*, Vol. 27, No. 7, 2005, pp. 790–800.

[26] Fayyad, U., Piatetsky-shapiro, G., and Smyth, P., "From data mining to knowledge discovery in databases", *Artificial Intelligence (AI) magazine*, Vol. 17, No. 3, 1996, pp. 37–54.

[27] Lan, H., *Data Mining: Practical machine learning tools and techniques*, 3rd ed., Morgan Kaufman, Boston, MA, 2011.

[28] Fe-Safe *User's Manual - Safe Technology Limited*, Sheffield, S10 2PQ, UK, 2011.

[29] Fisher, R.A., *Statistical Methods for researcher Workers*,Oliver and Boyd, London, UK,1925.

[30] Bolboacă, S. D., and Jäntschi L., "Design of experiments: Useful orthogonal arrays for number of experiments from 4 to 16." *Entropy*, Vol. 9, Nol.4, 2007, pp. 198-232.

[31] Taguchi, G., Jugulum, R., and Taguchi, S., *Computer-based robust engineering: essentials for DFSS*, ASQ Quality Press, Milwaukee, WI, 2004.